Differential impacts of drought and esca expression on Ascomycota fungi in the trunks and young organs of mature grapevines

Pierre GASTOU[1,2], Giovanni BORTOLAMI[1,3], Nathalie FERRER[1], Gregory A. GAMBETTA[4], Samuele MORETTI[1], Jessica VALLANCE[1], Chloé E.L. DELMAS[1,*]

[1] SAVE, INRAE, Bordeaux Sciences Agro, ISVV, F-33882 Villenave d'Ornon, France

[2] Département Sciences de l'Environnement, Univ. Bordeaux, F-33405 Talence, France

[3] Present address: Plant Ecology Research Laboratory PERL, School of Architecture, Civil and Environmental Engineering ENAC, EPFL, CH-1015 Lausanne, Switzerland.

[4] EGFV, Bordeaux Sciences Agro, Univ. Bordeaux, INRAE, ISVV, F-33882 Villenave d'Ornon, France

*Corresponding author: chloe.delmas@inrae.fr

Author contributions: C.E.L.D., G.A.G. and G.B. conceived the experimental drought x esca study; G.B. and N.F. sampled the tissues and ground the samples; G.B. analyzed the trunk section images; N.F. extracted DNA and performed PCR; P.G and J.V processed the bioinformatics pipeline; P.G. analyzed the data; S.M. contributed to the discussion section and to data interpretation; P.G wrote the first draft of the paper under the supervision of C.E.L.D.; All authors critically revised and approved the final version of the manuscript for submission.

Abstract

Perennial plant decline is increasingly threatening the profitability and sustainability of agriculture and forestry worldwide. It results from intricate interactions between microbial communities, the plant host, and abiotic stressors. We investigated the effects of drought and esca disease on mature grapevine phytobiomes. Grapevines display no esca leaf symptoms during droughts, but the impacts of drought and esca expression on fungal communities and wood health in mature plants remain poorly understood.

We studied 43 uprooted 30-year-old naturally infected vines in three experimental conditions: well-watered asymptomatic (Control) vines, vines with esca symptoms (Esca), and vines subjected to water deficit (WD) over two consecutive summers. We profiled trunk, cane, stem and petiole Ascomycota communities by DNA metabarcoding with primers specifically designed for grapevine trunk-associated Ascomycota, and quantified wood necrosis.

The Ascomycota communities of trunks and younger organs clearly differed, and drought and esca had different impacts on the Ascomycota communities of perennial and young organs. In the trunk, drought significantly decreased fungal diversity in healthy wood and increased the abundance of wood pathogens (e.g. *Phaeomoniella chlamydospora, Botryosphaeria dothidea*). In young organs, esca expression decreased the species richness and diversity of the Ascomycota community to a greater extent than drought. We also found that the relative proportion of healthy wood was smaller in plants with esca symptoms than in asymptomatic plants.

Thus, drought increased Ascomycota pathogen abundance in the trunk but did not increase wood degradation and esca expression, highlighting the need to investigate the molecular basis of plant-microbiome interactions under multi-stress conditions.

Keywords: Ascomycota communities, drought, esca, grapevine, metabarcoding, perennial plant decline, wood integrity

Introduction

A balanced plant microbiota is essential to preserve plant health and productivity in a context of global changes and emerging biotic pressures (Compant et al. 2019; Trivedi et al. 2020, 2022). The disequilibrium or dysbiosis of endophytic microbiota has been associated with plant dieback, although the causal mechanism is generally unknown (Arnault et al. 2023, Bettenfeld et al. 2020, Broberg et al. 2018, Griffiths et al. 2020). Pathogenic and saprotrophic species that are present in a latent endophytic phase within healthy plants (Hallmann et al. 1997, Marsberg et al. 2017) are often overabundant or more active in symptomatic plants, potentially worsening the decline of these plants (Bettenfeld et al. 2020, Jiao et al. 2023).

Plant microbial communities are also affected by abiotic factors, and these interactions are associated with plant dieback events worldwide (Ciesla and Donaubauer 1994, Desprez-Loustau et al. 2006, Manion 1981). In a context of climate change, the interactions of drought with plant physiology, plant pathogens and the whole microbial community (i.e. holobiont) are a major issue that cannot be reduced to unequivocal relationships. Depending on plant host species and physiological status, pathogen lifestyle, and the intensity and timing of the stress, drought may exacerbate, inhibit or have no effect on plant-pathogen interactions (Desprez-Loustau et al. 2006, Jactel et al. 2012, Luna et al. 2025, Ramegowda and Senthil-Kumar 2015, Torres-Ruiz et al. 2024). The impact of drought stress on phytobiomes has been documented principally for the rhizosphere and the phyllosphere (Bechtold et al. 2021, Fitzpatrick et al. 2018, Jaeger et al. 2024, Xu et al. 2018) but remains largely unknown for other compartments (e.g. endosphere or woody perennial organs). A comprehensive understanding of the interactions between perennial plant phytobiomes, abiotic and

biotic stresses would contribute to deciphering the relative roles of the various factors in plant decline.

Grapevine (*Vitis vinifera* L.), a major cultivated perennial crop, is particularly severely affected by complex dieback processes, mostly involving interactions between trunk diseases and environmental factors (Claverie et al. 2020, Etienne et al. 2024). Esca is a trunk disease causing grapevine dieback worldwide, with harmful consequences for the productivity and perenniality of the vineyard (Gramaje et al. 2018). Esca triggers physiological modifications in the leaf, stem and whole plant, impairing growth, hydraulic conductivity, gas exchange, and metabolism within perennial and vegetative organs (Bortolami et al. 2019, 2021a,b, 2023, Dell'Acqua et al. 2024a, Magnin-Robert et al. 2016, 2017). This disease is detected in the summer on plant canopies displaying typical symptoms of scorching between the veins of the leaf (so-called "tiger-stripe" symptoms) and apoplexy, which may be observed on some or all of the stems of plants randomly distributed over the vineyard (Lecomte et al. 2024). Internal wood necrosis, with black necrotic tissue and white rot, is observed in both symptomatic and asymptomatic plants (Bertsch et al. 2013). However, white rot tends to be more frequent in symptomatic plants (Bruez et al. 2020, Maher et al. 2012). The trunk microbiota differs between necrotic and non-necrotic (healthy) wood tissues (Bruez et al. 2020, Elena et al. 2018). In particular, black necroses are characterized by a high abundance of Ascomycota whereas white rot necrosis is caused by Basidiomycota fungi, such as *Fomitiporia mediterranea* (Bruez et al. 2020; Moretti et al. 2021). Conversely, there is no clear difference between the microbial communities of healthy wood collected from plants with and without esca leaf symptoms (Del Frari et al. 2019, Dell'Acqua et al. 2025, Hofstetter et al. 2012, Monod et al. 2024). Several environmental factors are typically involved in perennial plant dieback but drought has

a particularly strong impact in viticulture, and this impact is growing even stronger with the acceleration of climate change (van Leeuwen et al. 2024). In this context, the impact of drought on esca pathogens is a growing matter of concern, as both drought and esca have deleterious effects on grapevine hydraulic function.

Recent advances have improved our understanding of the environmental drivers of esca symptom expression, highlighting the key role of drought through its impact on plant water status. Contrasting with the many observations of synergistic drought-pathogen interactions in trees (Desprez-Loustau et al. 2006, Gomez-Gallego et al. 2022, Torres-Ruiz et al. 2024), esca and drought are antagonist in grapevine, inhibiting each other. Bortolami et al. (2021b) demonstrated that uprooted naturally infected plants subjected to moderate drought (predawn water potential around -1 MPa) did not express esca leaf symptoms at any time in the course of a two-year experiment. Dell'Acqua et al. (in press) showed that vines with esca symptoms are less affected by intense drought stress and recover more quickly after such stress. The characteristics of fungal communities probably play a key role in drought-esca interactions, but this role has never been elucidated in mature plants.

Drought modifies the structure and functioning of plant microbial communities across compartments (see for example Carbone et al. 2021, Debray et al. 2022; Lin et al. 2023, Trivedi et al. 2022). A recent pluriannual study on young potted vines revealed a significant shift in wood fungal communities during drought, with a decrease in the complexity of microbiota structure and interactions, and an increase in the abundance of *P. chlamydospora*, a pathogenic Ascomycota involved in Petri disease that has been implicated in the esca pathosystem (Leal et al. 2024). These results seem to contradict the antagonism between drought and esca. There is therefore a need to

131 validate these findings on mature grapevines and to consider again which Ascomycota
132 pathogens are associated with the different disease symptoms.

133

134 Here, we studied the effects of abiotic (drought) and biotic (esca) stresses on
135 Ascomycota communities in the various organs of grapevine. We addressed the
136 following questions: (i) What impact do seasonal drought and esca leaf symptom
137 expression have on the Ascomycota communities in trunk and younger vegetative
138 organs? (ii) Is the antagonistic relationship between esca and drought associated with
139 shifts in the functional properties of Ascomycota communities? (iii) How do drought
140 and esca expression affect internal wood necrosis and the corresponding Ascomycota
141 communities? We used the same 43 uprooted vines with different esca histories and
142 exposure to contrasting water conditions as described by Bortolami et al. (2021b). We
143 sampled the trunk (separating the necrotic and healthy wood) and young organs (two-
144 year-old canes, current-year stems, and petioles), and used a metabarcoding
145 approach to study grapevine trunk-associated ascomycete fungi.

146

147 **Materials and methods**

148

149 **Plant material and sampling.** Sampling was conducted between October 7 and 14
150 2019 on a subset of uprooted vines (*V. vinifera* L. cv. Sauvignon blanc; *n*=43) from the
151 experimental design described in detail by Bortolami et al. (2021b). This experimental
152 design included three factors: (i) two levels of watering regime in two consecutive
153 summer seasons in 2018 and 2019: WW (well-watered for two years, Ψ_{PD} close to 0
154 MPa), and WD (water-deficit, presenting $\Psi_{PD} \approx -1$ MPa from July to October in 2018
155 and 2019); (ii) two contrasting histories of esca symptoms since 2012: pA (previously

156 asymptomatic, i.e. plants that had never expressed esca leaf symptoms at any time
157 since 2012), and pS (previously symptomatic, i.e. plants that had expressed esca leaf
158 symptoms at least once since 2012); iii) two canopy phenotypes in 2019: presence of
159 esca leaf symptoms (typical tiger-stripe symptoms) and asymptomatic plants
160 (hereafter referred to as control plants). Plants subjected to a WD never expressed
161 esca leaf symptoms (see Bortolami et al. 2021b). We therefore sampled vines from
162 four distinct groups (Table 1): Water Deficit-pS (WD, *n*=12 asymptomatic plants in
163 2019); Esca-pS (Esca, *n*=10 well-watered plants expressing tiger-stripe symptoms in
164 2019); Control-pA (*n*=10, well-watered plants asymptomatic since 2012); Control-pS
165 (*n*=11, well-watered plants asymptomatic in 2019). Esca history had no significant
166 effect (see the Results section), so the Control-pA and Control-pS groups were
167 merged into a single control category (*n*=21, well-watered plants asymptomatic in
168 2019) for some analyses. During the growing seasons, the plants were regularly
169 treated for powdery mildew (with 80% micronized sulfur-based multisite products).
170 We sampled four different organs from each plant for DNA metabarcoding
171 (Table 1; Fig. S1): petioles (several petioles pooled together), stems from the current
172 year (one debarked internode from the middle of the stem), two-year-old canes (one
173 debarked internode), and trunks (with the separation of necrotic and healthy wood).
174 Consequently, both endophytic and epiphytic Ascomycota communities were included
175 in petiole analyses but only endophytic Ascomycota communities were included in the
176 analyses of woody organs (i.e. stems, canes, trunks). For plants expressing esca
177 symptoms, we separated petioles, stems and canes according to their disease status:
178 asymptomatic (AS) or displaying tiger-stripe symptoms on the leaves (S) (see pictures
179 of leaves in Fig. S1).
180

181 We used sterilized tools to remove the bark from the trunk of all plants. We
182 searched for the presence of a brown stripe, a colored band of xylem band appearing
183 under the bark concomitantly with esca leaf symptoms (Lecomte et al. 2012, 2024). A
184 brown stripe was observed in all the plants presenting leaf symptoms (Fig S1) but
185 none of the asymptomatic plants. We sampled chips from the brown stripe at different
186 heights along the trunk to obtain sufficient material. We then cut a 2 cm-thick cross-
187 section of the trunk 15 cm from the top of the plant and photographed it for further
188 analyses (Fig. S1). We collected tissue of different wood types from this cross-section
189 (after removal of the bark) with sterile shears in a sterile field. This tissue was
190 immediately immersed in liquid nitrogen and stored at -80°C. We collected the
191 following wood types (Table 1): apparently healthy wood, black necrotic wood, white
192 rot, and brown stripe. For white rot, if insufficient necrotic tissue was collected for
193 pathogen detection, we sampled additional white rot tissues from just above or below
194 the cut section. Necrotic tissue was sampled only when present, whereas healthy
195 wood was sampled from every plant. We obtained a total of 251 samples (Table 1):
196 134 young organs (48 petioles, 47 stems, 39 canes) and 117 trunks (43 healthy wood,
197 36 black necrosis, 29 white rot, and 9 brown stripes).
198
199 **DNA extraction and sequencing.** Samples (*n*=251) were ground in liquid nitrogen
200 with a one-ball mill TissueLyser II (Qiagen, Hilden, Germany), taking care to sterilize
201 the balls and sample holders with ethanol 70% between samples. Genomic DNA was
202 extracted from 60 mg wood tissue samples with the Indvisorb Spin Plant mini Kit
203 (Invitek Diagnostics, Berlin, Germany) according to the manufacturer's instructions.
204 Empty tubes — containing only the extraction reagents, without sample — were
205 included as negative controls for DNA extraction (*n* = 5). DNA was then quantified with

206 a DS-11 spectrophotometer (DeNovix, Wilmington, USA) and adjusted to a uniform
207 concentration of 15 ng.μl^{-1}. The ITS2 region of the nuclear ribosomal repeat unit was
208 then amplified with the GTAAf/GTTAr primers
209 (AAAACTTTCAACAACGGATC/GACCTCGGATCAGGTAGGRA), which were
210 specifically designed and optimized for the profiling of pathogenic Ascomycota fungal
211 communities associated with trunk diseases (Morales-Cruz et al. 2018b). DNA was
212 amplified by PCR with an Epgradient Mastercycler (Eppendorf, Hambourg, Germany)
213 in a reaction mixture (25 µl final volume) consisting of 1 µl DNA template (15 ng.µl-1),
214 10 µl of 2X Platinum Hot Start PCR Master Mix (Invitrogen,Waltham, USA), 0.5 µl of
215 each primer (10 µM), 1.25 µl 20X bovine serum albumin (New England BioLabs,
216 Ipswich, USA), and 11.75 µl DNAse/RNAse-free sterile water. The cycling parameters
217 were as follows: enzyme activation at 95°C for 2 min; 35 cycles of denaturation at 95°C
218 for 45 s, 60°C for 1 min, 72°C for 1.5 minutes; and a final extension at 72°C for 10 min.
219 Empty wells on the PCR plate — i.e. those containing the PCR mix but without
220 template — were used as negative controls (*n* = 9). The PCR products were visualized
221 by electrophoresis in a 2% agarose gel in TBE (molecular weight ≈350 bp). They were
222 then sent to the PGTB sequencing facility (Genome Transcriptome Facility of
223 Bordeaux, Pierroton, France) for sequencing on an Illumina MiSeq platform (v3
224 chemistry, 2x300 bp). PCR product purification, the addition of multiplex identifiers and
225 sequencing adapters, library sequencing and sequence demultiplexing (with exact
226 index search) were performed by the sequencing service, who included another five
227 negative PCR control samples at this stage.
228
229 **Sequence analysis and OTU table construction.** Metabarcoding data were
230 processed with the FROGS pipeline (Find Rapidly OTUs with Galaxy Solution)

231 implemented on a Galaxy instance (https://vm-galaxy-prod.toulouse.inra.fr/galaxy/;
232 Escudié et al. 2018). In brief, VSearch was used to merge paired reads with a
233 maximum of mismatch of 10% in the overlapping region. After denoising (i.e. reads
234 with no expected length - between 150 and 590 bp - and containing ambiguous bases,
235 N, were discarded) and the removal of primers/adapters removal with CUTADAPT
236 (Martin 2011), clustering was performed with SWARM (Mahé et al. 2014), with an
237 aggregation distance *d* = 1. Chimeras were removed and low-abundance sequences
238 were filtered out at 0.00005% (i.e. we retained OTUs accounting for at least 0.00005%
239 of all sequences, adapted from Bokulich et al. 2013), to discard singletons from the
240 datasets. The ITS2 region was extracted with ITSx (Bengtsson-Palme et al. 2013)
241 before determining the taxonomic affiliation of the fungal OTUs by BLAST queries
242 against the UNITE Fungi v8.2 (implemented in FROGS), trunkdiseaseID.org
243 (http://www. grapeipm.org/), and NCBI (nr/nt) nucleotide collection
244 (https://blast.ncbi.nlm.nih.gov/Blast. cgi) databases.
245 We performed a decontamination step, based on 19 DNA extraction and PCR
246 blanks, with the *metabaR v.1.0.0* package (Zinger et al. 2021) implemented in R
247 v.4.2.1 software. Graphical and statistical methods were used to flag and selectively
248 remove non-Ascomycota, putatively contaminating or artifactual OTUs, and potentially
249 unusable samples (i.e. highly contaminated or low sequencing depth).
250
251 **Metabarcoding statistical analysis.** We compared the diversity, structure and
252 composition of Ascomycota communities (see metrics below) between different
253 categories (Table 1): (i) organs (trunk, cane, stem, petiole; n = 251 samples),
254 considering plant status as a covariate; (ii) plant statuses in healthy trunk wood
255 samples; n = 43); (iii) plant statuses and organ statuses in young organs (n = 134); (iv)

256 trunk wood types (i.e. healthy wood, black necrosis, white rot, brown stripe; n = 117),
257 considering plant status as a covariate; (v) esca symptom histories (i.e. previously
258 asymptomatic *vs*. previously symptomatic) in control plants, considering plant status
259 as a covariate. The (v) analysis was performed separately on trunk (n = 51) and young
260 organ (n = 58) samples. For all analyses, we checked the normality of the residuals
261 (QQ-plot) and the homogeneity of the residual variance (residuals vs. fitted, residuals
262 vs. predictors) graphically. Non-parametric analyses were performed if these
263 assumptions were not satisfied. All analyses were performed with R v.4.2.1 and with
264 an alpha risk of 5%.

265 To estimate the diversity, structure and composition of Ascomycota
266 communities we calculated three alpha-diversity indices (i.e. observed richness,
267 Shannon index, Simpson index) with the "estimate_richness" function in *phyloseq*
268 *v.1.42.0* package (McMurdie and Holmes 2013), and compared them across
269 categories by ANOVA procedures followed by Tukey's post-hoc tests. For Simpson
270 index, the normality assumptions were not fulfilled, so we performed non-parametric
271 alternatives (i.e. Kruskal-Wallis test followed by Dunn's test). We subjected the
272 Ascomycota community structure of the samples to principal component analysis
273 (PCA) based on a redundancy dependence analysis (RDA) ordination on centered
274 log-ratio (CLR, recommended for compositional data; Gloor et al. 2017)-transformed
275 data, with the *phyloseq* "ordinate" function. We performed a permutational analysis of
276 variance (PERMANOVA) on CLR-transformed data, with the "adonis2" function in the
277 *vegan v.2.6-4* package (Oksanen et al. 2022), to assess the effect of organ, plant
278 statuses, or trunk wood type on Ascomycota community structure, with plant status
279 included as a covariate. The multivariate homogeneity of group dispersions was
280 checked *a posteriori*, and multilevel pairwise comparisons were calculated with the

281 “pairwise.adonis2” function in *pairwiseAdonis v.0.4.1* (Arbizu 2025). A pseudocount of
282 one was added to all OTU counts to handle zero values before CLR transformation,
283 thereby ensuring numerical stability during log-ratio calculations.

284 For some analyses, we classified Ascomycota OTUs into three groups
285 according to function: putative grapevine wood pathogens, putative antagonists of
286 grapevine wood pathogens (tested with success *in vitro*, in the greenhouse or in the
287 vineyard), and other taxa. This taxonomic classification to genus level was based on
288 the available scientific literature (Supplementary Table S1). The effect of plant status,
289 or wood type on these functional classes was evaluated by ANOVA followed by
290 Tukey’s post-hoc tests.

291 We performed differential analysis with linear discriminant analysis effect size
292 (LEfSe) to identify the Ascomycota species most likely to explain differences between
293 wood types, with the “run_lefse” function in the *microbiomeMarker v.1.4.0* package
294 (Cao et al. 2022) and the following parameters: kw_cutoff = 0.05 and lda_cutoff = 2.
295 We performed a differential analysis with the Aldex2 procedure to identify the
296 Ascomycota species most likely to explain differences between control and Esca
297 plants, and between control and WD plants. In this case, the “run_aldex” function was
298 applied to RLE-transformed data, with a *p*-value cutoff of 0.05.

299

300 **Analysis of trunk necrosis.** We used ImageJ software (Schneider et al. 2012) to
301 analyze each trunk cross-section image. We measured the area of apparently healthy
302 wood, black necrosis, and white rot (in mm^2) relative to the entire cross section. The
303 brown stripe was not visible on the cross sections because it affects only the outermost
304 xylem rings and was not, therefore, quantified as for the other tissues.

305 We assessed the effect of plant status (control, esca, WD) on the relative
306 proportions of healthy wood, black necrosis and white rot in trunk cross sections (n =
307 43). The effect of plant status on the statistical distribution of wood type proportions
308 was assessed with Fisher's exact test (simulated *p*-value, 2,000 replicates). The effect
309 of plant status on the proportion of each type of necrosis was assessed by ANOVA
310 followed by Tukey's post-hoc tests with "HSD.test" in the *agricolae v.1.3-7* package
311 (de Mendiburu 2023). We then plotted the statistical distribution of healthy wood and
312 compared it across plant statuses, using the minimal proportion of healthy wood in
313 control plants as a threshold. Finally, we assessed the effect of esca symptom history
314 on the proportion of each type of necrosis in control plants (n = 21).
315
316 **Results**
317 **General description of the Ascomycota community and differences between**
318 **organs.** In total, 10,765,305 reads were generated and assigned to 320 operational
319 taxonomic units (OTUs) (Supplementary Tables S2 and S3). The final decontaminated
320 dataset contained 9,641,320 reads (i.e. 10.4% of reads were removed) from 251 plant
321 samples that were affiliated to 297 OTUs (i.e. 7.2% were removed). Ascomycota
322 communities were composed of four main classes: Dothideomycetes (59.5%),
323 Eurotiomycetes (19.0%), Sordariomycetes (18.4%) and Leotiomycetes (2.2%). Less
324 than 1% of OTUs were affiliated to multiple classes or to no class. Global metrics for
325 both the raw and decontaminated datasets are provided in Supplementary Table S2.
326 The decontaminated OTUs are presented in Supplementary Table S3. The number of
327 reads per sample after decontamination and sample metadata are provided in
328 Supplementary Table S4.
329

330 We compared the diversity and structure of Ascomycota communities between
331 plant organs (i.e. trunk, cane, stem, petiole) across all samples. Shannon and Simpson
332 indices differed significantly between organs, whereas observed richness did not (P =
333 0.005, $P = 10^{-4}$ and P = 0.10, respectively). Ascomycota richness and diversity were
334 slightly lower in trunk samples than in other organs (Supplementary Fig. S2A). PCA
335 and PERMANOVA analyses revealed that organ accounted for 21% of the variance
336 of the total Ascomycota community (P = 0.001). Trunk samples were clearly separated
337 from canes, stems and petioles (Supplementary Fig. S2B). We therefore decided to
338 compare trunk samples and young organ samples (canes, stems and petioles,
339 corresponding to organs that were no more than two years old) in subsequent
340 analyses.
341
342 **Effects of drought and esca on the Ascomycota community in healthy trunk**
343 **wood samples.** Three species predominated in healthy trunk wood samples:
344 *Phaeomoniella chlamydospora* (28.2%), *Cladosporium sphaerospermum* (13.0%) and
345 *Phaeoacremonium minimum* (8.1%; Fig. 1A). Plant status significantly influenced the
346 Shannon and Simpson indices of healthy wood but not observed richness (P = 0.01,
347 P = 0.04 and P = 0.17, respectively). Ascomycota diversity was significantly lower in
348 the healthy wood of WD plants than in that of control plants, whereas it did not differ
349 significantly between esca and the other two experimental conditions (Fig. 1B). PCA
350 and PERMANOVA analyses revealed that plant status accounted for 6.9% of the
351 variance of the Ascomycota community in healthy wood (P = 0.001). WD plants
352 differed significantly from control plants, whereas esca plants were intermediate (Fig.
353 1C).
354

355 Plant status significantly affected the relative abundance of putative grapevine
356 wood pathogens and antagonists (Supplementary Table S1) in healthy wood, but did
357 not affect the abundance of other taxa (P = 0.006, P = 0.006 and P = 0.38, respectively;
358 Fig. 1D). The relative abundance of putative pathogens was significantly higher in WD
359 plants than in control plants (Fig. 1D), whereas the abundance of putative antagonists
360 was significantly lower in WD plants than in control plants (Fig. 1D).
361 Finally, Aldex2 differential analyses to identify Ascomycota species highlighted
362 differences in microbial composition between plants with different disease statuses.
363 One phylum-affiliated Ascomycota OTU was significantly less abundant in plants with
364 esca symptoms than in control plants. Four fungal species, including the pathogens
365 *P. chlamydospora* and *Botryosphaeria dothidea*, were significantly more abundant in
366 WD plants than in control plants. Conversely, four fungal species, including putative
367 antagonist *Cladosporium* spp. and *E. nigrum*, were significantly less abundant in WD
368 plants than in control plants (Fig. 1A; Supplementary Table S5).
369
370 **Effects of drought and esca on Ascomycota communities in young organs.** We
371 first looked for differences in the Ascomycota community between asymptomatic and
372 esca-symptomatic young organs from plants with esca symptoms. We found no
373 significant difference between these two groups of organs for either alpha-diversity or
374 beta-diversity metrics (Supplementary Table S6).
375 We then compared the Ascomycota communities in young organs between
376 control, esca (pooling samples from asymptomatic and symptomatic canes, stems and
377 petioles) and WD plants. Three species predominated in young organs: *Cladosporium*
378 *sphaerospermum* (44.5%), *Cladosporium halotolerans* (20.0%), and *Diaporthe*

379 *ampelina* (5.1%; Fig. 2A). The genus *Cladosporium* accounted for 69.1% of the OTUs
380 retrieved from young organs.

381 Plant status significantly influenced observed richness, and the Shannon and
382 Simpson indices ($P = 10^{-6}$, $P = 0.003$ and $P = 0.02$, respectively). Ascomycota diversity
383 was lower in the young organs of esca plants than in those of control and WD plants
384 (Fig. 2B). PCA and PERMANOVA analyses revealed that plant status accounted for
385 5.5% of the variance of the Ascomycota community in young organs ($P = 0.001$). In
386 pairwise comparisons, there were slight differences between plant statuses (Fig. 2C).

387 We performed Aldex2 differential analyses to identify the Ascomycota species
388 underlying the differences in microbial composition between the young organs of
389 plants with different disease statuses. *Erysiphe necator* was significantly more
390 abundant in esca plants than in control plants. Conversely, 12 fungal species,
391 including several putative antagonist *Cladosporium* spp. and *Aureobasidium pullulans*,
392 were significantly less abundant in esca plants than in control plants. Two fungal
393 species, *Exophiala* sp. and *B. dothidea*, were found to be significantly more abundant
394 in young organs from WD plants than in those of control plants. Conversely, six fungal
395 species, including several *Cladosporium* spp. and *Aureobasidium pullulans*, were
396 found to be significantly less abundant in WD plants than in control plants (Fig. 2A;
397 Supplementary Table S5). Overall, putative wood pathogens accounted for 11.8 ±
398 0.2% of the OTUs in young organs. These pathogens were slightly more abundant in
399 esca and WD plants than in control plants ($P = 0.05$). Putative antagonistic genera
400 accounted for 72.9 ± 0.2% of OTUs in young organs, and were less abundant in esca
401 and WD plants than in control plants ($P = 10^{-4}$).

402

403 **Effects of drought and esca on wood integrity**. We quantified the areas occupied
404 by apparently healthy wood, black necrotic wood and white rot in trunk cross sections
405 (Supplementary Table S7). The relative proportions of these three types of wood
406 differed significantly between plant statuses (i.e. control, esca and WD; $P = 10^{-4}$). The
407 proportion of healthy wood was significantly lower in plants with esca symptoms than
408 in control plants, but did not differ significantly between WD plants and the other two
409 categories (Fig. 3A). The proportions of black necrosis and white rot did not differ
410 significantly between plant disease statuses ($P = 0.10$ and $P = 0.12$, respectively), but
411 there was a trend towards a higher proportion of white rot in plants with esca symptoms
412 and a higher proportion of black necrosis in WD plants (Fig. 3A). In 60% of plants with
413 esca symptoms, the proportion of healthy wood was lower than the minimum value
414 recorded in control plants (34.3%).
415
416 **Ascomycota communities in trunk necrotic wood tissues.** We compared trunk
417 Ascomycota communities between apparently healthy wood, brown stripe, black
418 necrosis and white rot samples collected in October, several weeks after symptom
419 onset. Brown stripe samples were collected only from plants displaying esca
420 symptoms (Table 1) and the sample size is lower for this tissue type. Wood type
421 significantly affected alpha-diversity metrics, i.e. observed richness, and the Shannon
422 and Simpson indices ($P < 10^{-16}$, $P = 10^{-12}$ and $P = 10^{-6}$, respectively). Ascomycota
423 richness and diversity were lower in necrotic wood (i.e. black necrosis or white rot),
424 than in healthy wood and brown stripe (Fig. 3B). PCA and PERMANOVA analysis
425 revealed that wood type accounted for 11.9% of the variance of the Ascomycota
426 community in a model including plant status and wood type * plant status as covariates
427 ($P = 0.001$). All pairwise comparisons between wood types were significant, but the

428 clearest difference was that between necrotic and non-necrotic areas (Fig. 3C). The
429 interaction between wood type and plant status was not significant: the differences in
430 Ascomycota communities between non-necrotic and necrotic wood were observed in
431 control, esca or WD plants (Supplementary Fig. S3).

432 Classifying Ascomycota OTUs into putative wood pathogens, antagonists and
433 others (Supplementary Table S1), we found that wood type significantly modified the
434 relative abundance of putative wood pathogens and putative antagonists, but not of
435 other taxa ($P = 10^{-15}$, $P = 10^{-10}$ and $P = 0.16$, respectively; Fig. 4A). The abundance of
436 putative pathogens was higher within the areas of black and white rot than in healthy
437 wood (Fig. 4A). The abundance of putative antagonists was high in healthy wood and
438 brown stripe, whereas these fungi were almost entirely absent from necrotic areas
439 (Fig. 4A). Finally, we performed a linear discriminant analysis to identify the
440 Ascomycota species driving the differences in microbial composition between wood
441 types. Six fungal species, including the putative antagonist of trunk pathogens
442 *Epicoccum nigrum,* were identified as biomarkers of healthy wood. Nine fungal species
443 were identified as biomarkers of brown stripe samples, including several pathogens
444 belonging to the Botryosphaeriaceae and putative antagonist *Cladosporium* spp.
445 Three fungal species were significantly associated with black necrosis, including the
446 pathogenic species *Phaeoacremonium minimum*. Four fungal species were
447 significantly associated with white rot, including the pathogenic species *Phaeomoniella*
448 *chlamydospora* and several *Penicillium* spp. (Fig. 4B).

449

450 **Effects of esca history on wood necrosis and Ascomycota communities.** We
451 assessed the effect of esca history on the distribution of wood types and the properties
452 of Ascomycota communities in control plants. Esca history (comparing pS and pA

453 plants with plant status as a covariable) had no significant impact on the distribution
454 of wood types (healthy wood, black necrosis and white rot) in trunk cross sections
455 (Supplementary Table S8).
456 In addition, the Ascomycota community in healthy trunk wood and young organ
457 samples did not differ significantly between pA and pS plants in terms of either alpha-
458 diversity or beta-diversity metrics (Supplementary Table S8).
459
460 **Discussion**
461
462 Disentangling the complex interplay between plants, microbial communities and
463 abiotic stresses is crucial for understanding the processes underlying perennial plant
464 decline. In this study, we used a unique experimental design to characterize plant and
465 Ascomycota community responses to esca disease and drought stress in mature
466 grapevines. We extended the work of Bortolami et al. (2021b) showing that the
467 expression of esca symptoms is inhibited by drought under controlled conditions, using
468 naturally infected plants. We sampled the plants at the end of the experiment and
469 demonstrated that the impact of drought on Ascomycota communities was greatest in
470 the trunk, whereas the expression of esca symptoms affected mostly younger organs.
471 The esca-drought antagonism revealed by Bortolami et al. (2021b) is not related to a
472 decrease in the abundance of grapevine wood pathogens. Finally, we demonstrated
473 that the incidence of esca symptoms on leaves was associated with a significant
474 decrease in the relative proportion of apparently healthy (i.e. non-necrotic) wood in the
475 trunk, with a corresponding increase in the proportion of necrotic tissues with a low
476 diversity of Ascomycota and a high abundance of wood pathogens.
477

Drought favors the pathogenic component of the Ascomycota community in trunk healthy wood whereas esca does not. In this study, the endophytic Ascomycota community in the healthy wood of the trunk was particularly strongly affected by intense drought stresses applied during two consecutive summers, whereas the seasonal expression of esca leaf symptoms affected the Ascomycota within young organs. The impact of drought has been studied in belowground communities in particular (e.g. Carbone et al. 2021, Jaeger et al. 2024), but drought can also shape endophytic microbial communities, by (i) directly affecting the living environment of fungi, by decreasing xylem water potential and humidity (Aung et al. 2018, Luard and Griffin 1981, Dell'Acqua et al., in press) and (ii) modulating microbe-microbe and plant-microbe interactions (Trivedi et al. 2020). We found a low diversity of Ascomycota in healthy trunk wood under drought conditions. This finding is consistent with the results of Leal et al. (2024), who used one-year-old grapevine cuttings to demonstrate a substantial decrease in microbial interactions, thereby providing evidence in support of a drought-induced microbial imbalance. The effects of drought stress on plant and microbial communities include osmotic shock and the generation of reactive oxygen species (ROS; Schimel et al., 2007; Miller et al., 2010, Singh et al., 2011). Under drought conditions, the Ascomycota community in the trunk may shift towards specific taxa with more efficient intracellular ROS scavenging mechanisms and an ability to produce compatible osmolytes. The relative abundance of Ascomycota wood pathogens, including *Phaeomoniella chlamydospora* in particular, increased in the trunk under water deficit conditions, even in the absence of foliar symptoms on water-stressed plants (Bortolami et al. 2021b). The increase in *P. chlamydospora* levels under drought conditions has been reported before (Hrycan et al. 2025, Leal et al. 2024). It may be due to a change in fungal interactions, with an

503 increase in the abundance of competitive species and their activities under drought,
504 and a greater adaptation of *P. chlamydospora* to a constrained environment (i.e. in the
505 presence of activated plant defenses and a low water potential) potentially favoring its
506 development at the expense of its usual antagonists and competitors. Interestingly, *P.*
507 *chlamydospora* seems to cope well with the oxidative stress induced by plant cells due
508 to its efficient ROS scavenging arsenal (Fischer et al., 2016). However, this finding is
509 more surprising given that the foliar expression of esca symptoms was inhibited under
510 drought conditions.

511 Interestingly, during the years following rewatering, the WD plants kept alive
512 had a probability of expressing esca leaf symptoms similar to that of control plants (C.
513 Delmas, personal communication). The increase in *P. chlamydospora* abundance did
514 not lead to a higher incidence of symptoms in subsequent years. The total wood
515 pathogen load appeared to be higher in plants expressing esca, due to the presence
516 of larger necrotic areas rich in pathogens. However, the observation that these
517 pathogens are not more abundant in the healthy wood of symptomatic plants, where
518 the process of degradation leading to necrosis presumably occurs, raises questions
519 about the exact role of Ascomycota in esca pathogenesis. Ascomycota pathogens are
520 generally considered to play an important, if not essential role in the expression of
521 esca symptoms (e.g. Bertsch et al. 2013, Gramaje et al. 2018). However, relative
522 abundance, studied here through metabarcoding approaches, may not be the most
523 relevant trait. Instead, the activity of Ascomycota pathogens (e.g. *Phaeomoniella*
524 *chlamydospora*, *Botryosphaeriaceae* spp.), including their expression of virulence
525 factors, may decrease in water deficit conditions, or increase before the expression of
526 esca symptoms (Desprez-Loustau et al. 2006, Morales-Cruz et al. 2018a, Nerva et al.
527 2022). There is also growing scientific evidence to suggest that the contribution of

528 Ascomycota to esca expression is overestimated (Hofstetter et al. 2012, Nerva et al.
529 2022, Moretti et al. 2023). These results call for refining our knowledge of gene
530 expression and metabolic changes in both plants and pathogens in the context of
531 multiple stress experiments.

532 Drought did not significantly modify the proportion of necrotic wood, but it did
533 slightly decrease the white rot/black necrosis ratio. This suggests that drought may
534 interfere slightly with the activity of white-rot basidiomycetes that degrade wood
535 through both enzymatic and non-enzymatic decay pathways (Moretti et al. 2021,
536 2023). Drought has already been identified as a variable that may affect wood decay
537 (Jia et al. 2024). Indeed, to grow through the lignocellulose matrix and release their
538 arsenal of decay-mediating molecules (i.e. enzymes and low-molecular weight
539 compounds) into the wood cell wall, wood decay fungi (Basidiomycota included)
540 require the moisture content in the wood to be at least above the fiber saturation point
541 (Goodell 2020, Zaber and Morrell 2012). This highlights the importance of studying the
542 abundance and activity of Basidiomycota, but also of bacteria that can act in synergy
543 in the wood degradation process (Del Frari et al. 2021, Haidar et al. 2021).

544 The expression of esca symptoms did not significantly modify plant-microbiome
545 interactions in healthy trunk tissues (despite a trend towards lower species richness
546 and an increase in the abundance of wood pathogens) as reported in other studies
547 (Del Frari et al. 2019, Monod et al. 2024; Dell'Acqua et al. 2025). Very few studies
548 have quantified the impact of dieback diseases on endophytic communities in other
549 plants (e.g. Raghavendra et al. 2017, Steinrucken et al. 2016), although modifications
550 in belowground microbial diversity were highlighted (Darriaut et al. 2024, Farooq et al.
551 2022, Han et al. 2022, Lasa et al. 2024). Such modifications may be accompanied by
552 an ecological disequilibrium, with an increase in the pathogenic component and a loss

553 of beneficial functions, such as symbioses between plants and fungi and the promotion
554 of plant growth (Gómez-Aparicio et al. 2022, Ma et al. 2024, Solís-García et al. 2021).
555 Our findings confirm that esca is a complex pathosystem, in which plant physiology,
556 interacting with the abiotic environment, plays a key role in leaf symptom onset, without
557 any major change in fungal communities in healthy wood tissue.
558
559 **Esca induces a more significant shift in Ascomycota communities in young**
560 **organs than drought.** Two consecutive summer seasons under drought conditions
561 had a greater impact on the trunk than esca, but seasonal esca expression had a
562 greater effect on Ascomycota communities in younger organs, which undergo
563 significant physical, physiological and metabolic changes during the expression of
564 esca symptoms (Bortolami et al. 2021a,b, Dell'Acqua et al. 2024, 2025). The
565 Ascomycota communities inhabiting young organs (mainly endophytes, except for the
566 petioles, from which we sampled both endophytes and epiphytes) on plants displaying
567 esca symptoms were less diverse than those of control plants and were largely
568 dominated by *Cladosporium* species. This finding suggests that the presence of leaf
569 symptoms influences, albeit slightly, microbial communities distal to the infection zone
570 characterized by necrosis and abundant trunk pathogens (i.e. perennial organs). Leaf
571 endophytic fungal communities have been shown to be modified by esca expression
572 (Del Frari et al. 2025). Accumulation and qualitative changes have been reported for
573 primary and secondary metabolites (e.g. sugars, terpenes, flavonoids; Bortolami et al.
574 2021b, Del Frari et al. 2025, Weiller et al. 2024) in leaves and stems expressing esca
575 symptoms, and these effects may be greater than those observed in the trunk,
576 explaining the stronger response of fungal communities to esca expression in younger
577 organs. Moreover, biotic stresses (such as esca disease) also induce ROS generation,

578 and fungi have developed strategies for scavenging ROS (Lehmann et al. 2015).
579 Therefore, as discussed above for the trunk, Ascomycota communities in young
580 organs may shift towards specific taxa with more efficient ROS scavenging
581 mechanisms.

582 However, esca had only a small effect in our experiment and other studies
583 have revealed the stem microbial communities to be similar in asymptomatic plants
584 and plants with esca symptoms (Del Frari et al. 2019). Water deficit had an even
585 weaker effect on the Ascomycota communities of young organs, despite the highly
586 significant physiological impact of drought during the experiment (Bortolami et al.
587 2021b). The main physiological difference between the plants subjected to water
588 deficit and those expressing esca symptoms was that water potential was strongly
589 affected by drought but not by esca expression, despite both conditions decreasing
590 plant transpiration. Photosynthesis and the balance of non-structural carbohydrates
591 were more strongly affected by esca expression, with a decrease in leaf chlorophyll
592 content and an accumulation of monosaccharides in leaves and stems, at the expense
593 of sucrose production and starch storage (Bortolami et al. 2021b). The Ascomycota
594 communities in young organs may have been more sensitive to carbon resource
595 availability and the concentration of non-structural carbohydrates, whereas wood
596 water status may be ecologically more selective for trunk communities. Conversely,
597 these results demonstrate the resilience of the microbial communities in young aerial
598 organs to decreases in water potential during drought, with no significant decrease in
599 diversity and no increase in the abundance of specific ecological guilds. Finally, the
600 relative abundance of *E. necator*, the causal agent of grapevine powdery mildew, was
601 higher in asymptomatic vegetative organs on plants displaying esca symptoms,
602 potentially due to a slight increase in gas exchange in these specific organs (Bortolami

603 et al. 2021b). *E. necator* was less prevalent in organs expressing esca symptoms,
604 perhaps due to the impairment of carbon assimilation (Guilpart et al. 2017).
605
606 **On the relationship between wood necrosis, pathogens and the expression of**
607 **esca foliar symptoms.** The causal links between the internal consequences of plant-
608 pathogen interactions (i.e. wood necrosis) and the external expression of disease (i.e.
609 foliar symptoms) remain poorly understood in perennial plant decline (Claverie et al.
610 2020, Gosling et al. 2024, Skovsgaard et al. 2010). Esca foliar symptoms have been
611 reported to be associated with a higher proportion of wood necrosis, especially white
612 rot, in *Vitis vinifera* L. cv. 'Cabernet-Sauvignon' (Maher et al. 2012, Ouadi et al. 2019).
613 Consistent with these findings, we found that plants displaying esca symptoms had
614 significantly lower proportions of healthy wood in their trunks than control plants.
615 However, our results demonstrate that the proportion of healthy wood explained esca
616 symptom expression in *V. vinifera* cv. 'Sauvignon blanc' better than the type of
617 necrosis. This may reflect a cumulative loss of functional xylem area (i.e. of the active
618 tissues located in the outer xylem; McElrone et al. 2021) in symptomatic plants,
619 regardless of the type of degradation. The mean proportion of white rot was about 20%
620 in control plants (i.e. well-watered and asymptomatic in the year of sampling), higher
621 than in previous reports. As plant age and genotype are significant drivers of esca leaf
622 symptom expression (Etienne et al. 2024, Gastou et al. 2024), we can hypothesize
623 that these factors modulate the proportion of necrotic wood (Claverie et al. 2023). In
624 old plants (30-y-o in our study), control plants with an asymptomatic history had similar
625 necrosis extent and Ascomycota community in the trunk than previously symptomatic
626 plants. In addition to a threshold of necrotic wood proportion in the trunk, the area of
627 contact between active xylem tissue (efficiently transporting sap) and specific necrotic

628 tissues, or the activity of microbial communities (e.g. virulence factors) may be
629 involved in the onset of foliar symptoms and should be explored further.

630 In the classical model of plant-microorganism interactions underpinning esca
631 expression, Ascomycota fungi are considered to be responsible for black necrosis,
632 black spots, wood streaks and discoloration, whereas white rot is associated with
633 Basidiomycota wood-degrading species, probably in interaction with bacteria (Bertsch
634 et al. 2013, Bruez et al. 2020, Haidar et al. 2021, 2024, Moretti et al. 2021). However,
635 less attention has been paid to the relationship between the total microbiome and the
636 type and extent of necrosis and to the role of Ascomycota fungi in white rot
637 propagation. We show here that, whatever the health status of the plant (i.e. control,
638 Esca or water deficit), the necrotic areas in the trunk harbored less diverse
639 Ascomycota fungal communities than adjacent apparently healthy areas, confirming
640 the results obtained for cordons (Bruez et al. 2020). These areas were dominated by
641 Ascomycota wood pathogens, the proportion of which increased at the expense of
642 other taxa, including putative antagonists, as previously highlighted in grapevine trunk
643 diseases (Martín et al. 2022), but not in other pathosystems (Bakys et al. 2009,
644 Denman et al. 2016). We found that *Phaeoacremonium minimum* was clearly
645 overrepresented in black necrotic areas, whereas *Phaeomoniella chlamydospora* was
646 not. *P. chlamydospora* was significantly overrepresented in white rot tissues, as
647 previously reported by Bruez et al. (2020) and Pacetti et al. (2021). The previously
648 favored hypothesis of a pioneering role of Ascomycota fungi before Basidiomycota
649 species in the sequence of events occurring during the colonization of healthy
650 grapevine wood has recently been revisited in light of new findings on potential intra-
651 and extracellular machinery for the detoxification of wood phenolic compounds in
652 *Fomitiporia mediterranea* (Moretti et al. 2021, Schilling et al. 2022, Garcia et al. 2024).

653 For *P. chlamydospora* a hypothetical role in wood decay through the opportunistic
654 colonization of highly degraded areas or co-degradation, possibly alongside
655 Basidiomycota, therefore appears more plausible than the pioneer hypothesis.
656 Moreover, *P. chlamydospora* may be less closely associated with black necrosis, as
657 previously suggested (e.g. Bertsch et al. 2013, Surico et al. 2006). It is, in any case, a
658 very abundant endophyte in healthy tissues (Del Frari et al. 2019, Hofstetter et al.
659 2012; Dell'Acqua et al. 2025). Finally, we resequenced healthy wood samples, using
660 ITS markers to quantify Basidiomycota and determine their relative abundance in
661 healthy wood samples; we confirmed that *Fomitiporia mediterranea* was present at
662 high abundance in the wood of plants expressing esca symptoms (Chambard et al.,
663 submitted).

664 We also characterized the Ascomycota community associated with the brown
665 stripe xylem observed in plants with symptomatic esca about three months after the
666 onset of leaf symptoms. We showed that the Ascomycota community in this
667 symptomatic tissue is diverse and similar to that retrieved from healthy woody tissues.
668 This finding is consistent with the fact that the brown stripe has not yet become a
669 necrotic area. This tissue no longer conducts water, as shown by the use of a dye to
670 follow sapwood transport (Lecomte et al. 2024), and in other vascular pathosystems
671 (Agrios 2005, Bibuci and Cirulli, 2012, Jiménez-Díaz et al. 2012). The brown color
672 probably results from the translocation of oxidizing phytotoxins and degradation
673 products and is associated with non-gaseous vascular embolism (e.g. tyloses and
674 gels; Agrios 2005, Bubici and Cirulli, 2012, Lecomte et al. 2024). We confirmed the
675 very high abundance of Botryosphaeriaceae spp. in brown stripe tissues late in the
676 season (Larignon et al. 2001), alongside *Cladosporium* spp. However, these
677 observations were performed three months after symptom onset. We cannot therefore

draw any firm conclusions about the changes in plant-fungus interactions potentially leading to the co-occurrence of brown stripe and foliar symptoms. More detailed studies of the microbial and physiological features related to the brown stripe symptom, and of the temporal dynamics linking internal and external symptoms, are now required.

Conclusion. Overall, this experimental study provides a new perspective on the ways in which abiotic and biotic stresses can shape microbial communities in perennial plants and contribute to plant decline. The trunk and younger grapevine organs had different endophytic fungal communities with different responses to drought and esca. Only esca significantly altered wood integrity. However, we were unable to investigate the dual-stress situation, as water deficit inhibited the expression of esca foliar symptoms. Based on these findings, assessments of the responses of the grapevine holobiont to combinations of stresses at the physiological and microbiome levels across various cultivars appear relevant to identify promising genotypes in the context of climate change and perennial plant decline. Indeed, wood degradation (Arnold et al. 2025), the incidence of esca foliar symptoms (Gastou et al. 2024), drought tolerance (Dayer et al. 2022) and endophytic microbial communities (Bekris et al. 2021, Hamaoka et al. 2022) differ between grapevine genotypes. Finally, plant dieback is related not only to endophytic communities, but also to microbiomes inhabiting the soil compartment (Darriaut et al. 2021, 2023, Gómez-Aparicio et al. 2022, Lasa et al. 2024). Future holistic *in natura* microbiome studies (i.e. multidisciplinary, multicompartments and/or multitaxa) would be particularly helpful, providing precise and generalizable results on the response of the holobiont to stressful conditions.

Data availability. DNA sequencing datasets will be made available in the ENA database under the accession number PRJEB87388.

Acknowledgments

We would like to thank Elena Farolfi and Jérôme Pouzoulet for help with plant sectioning and wood sampling, and Corinne Vacher for advice on metabarcoding analyses.

Funding

This work was supported by (1) the French Ministry of Agriculture and Food, FranceAgriMer, and the *Comité National des Interprofessions des Vins à appellation d'origine et à indication géographique* within the PHYSIOPATH Project (22001150-1506; Program *Plan National Dépérissement du Vignoble*) and (2) the French government in the framework of the IdEX Bordeaux University "Investments for the Future" program / GPR Bordeaux Plant Sciences. PG was awarded a PhD by the French *Ministère de l'Enseignement Supérieur et de la Recherche*.

Competing Interests statement

The authors have no competing interests to declare.

List of supplementary material

Supplementary Fig. S1: Pictures of the sampling

Supplementary Fig. S2: Properties of Ascomycota communities in all samples (i.e. trunk, cane, stem and petiole samples) across organs.

727 **Supplementary Fig. S3:** Ascomycota community structure across wood types for
728 each plant status.
729 **Supplementary Fig.S2:** Properties of Ascomycota communities in all samples (i.e.
730 trunk, cane, stem and petiole samples) across organs.
731 **Supplementary Table S1:** Ascomycota genera classified as putative wood pathogens
732 and putative wood antagonists.
733 **Supplementary Table S2:** Global metrics describing the GTAA metabarcoding
734 dataset before and after the decontamination process.
735 **Supplementary Table S3:** OTU table corresponding to the entire decontaminated
736 GTAA metabarcoding dataset.
737 **Supplementary Table S4:** List of experimental factors and Ascomycota reads for
738 each sample included in the GTAA metabarcoding study.
739 **Supplementary Table S5:** Summary of the results obtained in Aldex2 differential
740 analyses in healthy trunk samples and young samples.
741 **Supplementary Table S6:** Statistical modelling of organ health status (S-AS vs S-S)
742 effects on alpha-diversity metrics and Ascomycota community structure computed for
743 young organs.
744 **Supplementary Table S7:** List of experimental factors and wood type percentages
745 for each plant
746 **Supplementary Table S8:** Statistical modelling of esca history (pA vs pS) effects on
747 the distribution of wood types and alpha-diversity metrics and Ascomycota community
748 structure computed for healthy trunk and young samples.
749

750 **Tables and figures**

751

752 **Table 1. Number of *Vitis vinifera* cv. Sauvignon blanc plants and samples**
753 **included in this study, classified by experimental plant status, organ and sample**
754 **types.** For esca plants, samples of petioles, current-year stems, and two-year-old
755 canes were classified by organ status: asymptomatic (AS) or presenting tiger-stripe
756 symptoms on the leaves (S). Plants were classified by esca history: previously
757 asymptomatic (pA) or previously symptomatic (pS).

Plant status – esca history	Nb of plants	Organ	Nb of samples (per sample type or organ status)
Control – pA	*N* = 11	Trunk	*n* = 22 (10 healthy; 6 black necrosis; 6 white rot)
		Cane	*n* = 9
		Stem	*n* = 9
		Petiole	*n* = 9
Control – pS	*N* = 10	Trunk	*n* = 29 (11 healthy; 10 black necrosis; 8 white rot)
		Cane	*n* = 10
		Stem	*n* = 11
		Petiole	*n* = 10
Esca – pS	*N* = 10	Trunk	*n* = 35 (10 healthy; 9 brown stripe; 8 black necrosis; 8 white rot)
		Cane	*n* = 9 (8 AS; 1 S)
		Stem	*n* = 14 (4 AS; 10 S)
		Petiole	*n* = 18 (10 AS; 8 S)
Water deficit – pS	*N* = 12	Trunk	*n* = 31 (12 healthy; 12 black necrosis; 7 white rot)
		Cane	*n* = 11
		Stem	*n* = 13
		Petiole	*n* = 11

758
759
760

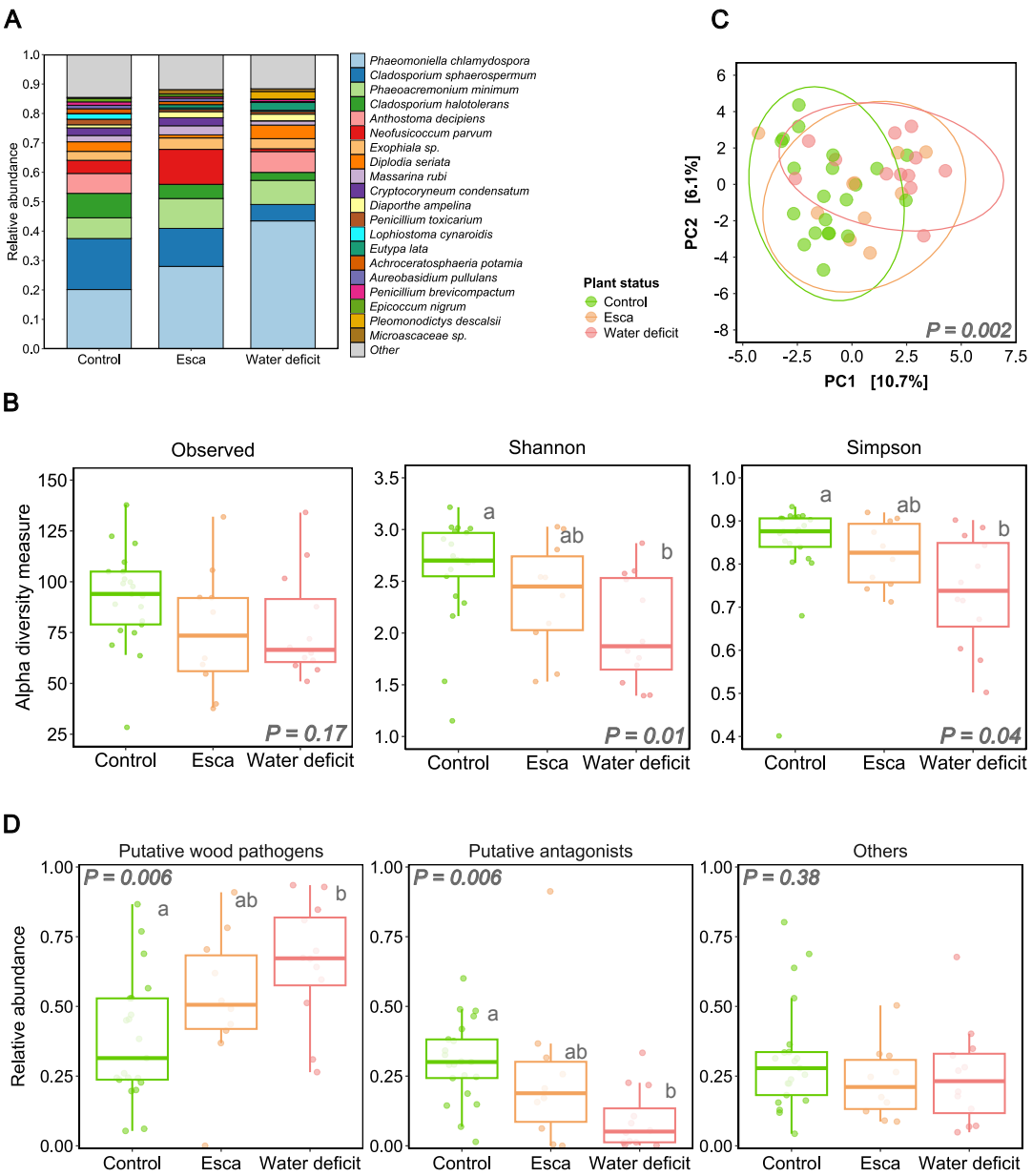

Fig. 1. Properties of endophytic Ascomycota communities in healthy trunk samples according to plant status

A, Distribution of the 20 most abundant Ascomycota OTUs in trunk samples, by plant status. The mean relative abundance was calculated for each OTU, by plant status. *Stacked bars are colored according to the OTU. Less abundant OTUs are grouped in the category "Other" and are colored in light gray.* **B**, Effect of plant status on alpha-diversity metrics (i.e. observed richness, Shannon and Simpson indices) associated

769 with Ascomycota communities. **B**, PCA summarizing the structure of Ascomycota

770 communities according to an RDA on CLR-transformed data. Ellipses correspond to

771 the 95% interval for each group. **C**, Relative abundance of putative wood pathogens,

772 putative antagonists and other taxa, by plant status. All graphs are colored according

773 to plant status.

774

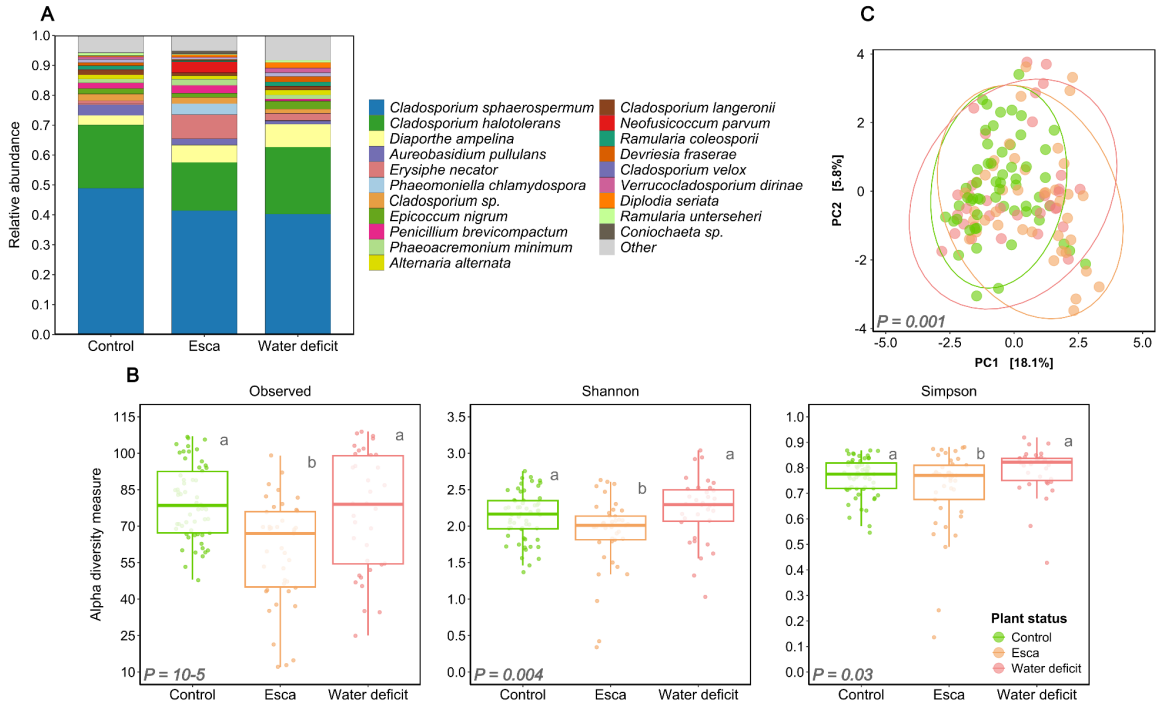

775

776 **Fig. 2. Properties of endophytic and epiphytic Ascomycota communities in**

777 **young organs (i.e. petioles, stems and canes), by plant status.**

778 **A,** Distribution of the 20 most abundant Ascomycota OTUs, by plant status, in young

779 samples. Mean relative abundances were calculated for each OTU, by plant status.

780 *Stacked bars are colored according to the OTU. Less abundant OTUs are grouped*

781 *into the "Other" category and colored in light gray.* **B**, Effect of plant status on alpha-

782 diversity metrics (i.e. observed richness, Shannon and Simpson indices) associated

783 with Ascomycota communities. **C**, PCA summarizing the structure of Ascomycota

784 communities according to an RDA on CLR-transformed data. Ellipses correspond to

785 the 95% interval for each group. Panels B and C are colored according to plant status.

786

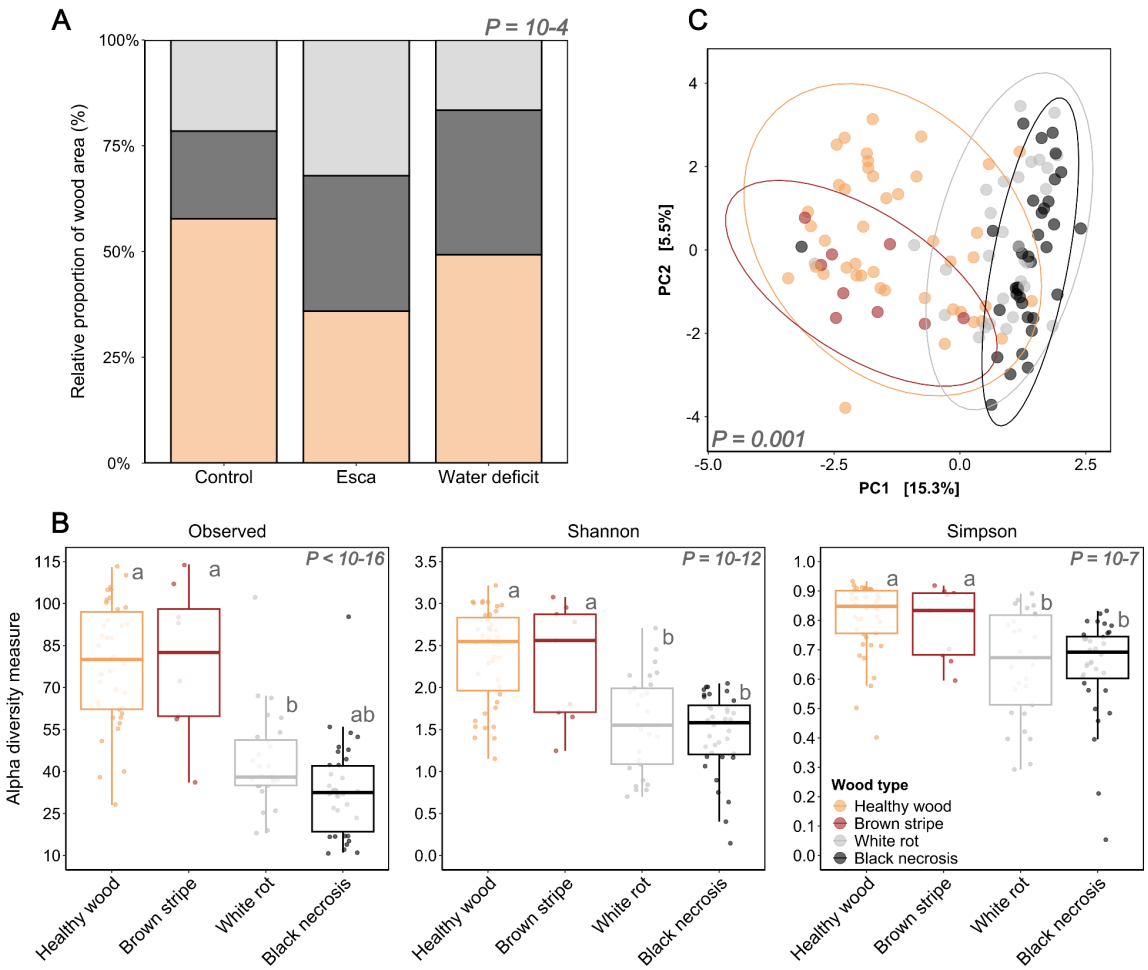

787

788 **Fig. 3. Relative proportions of wood symptoms in trunk cross-sections**

789 **according to plant status (control, esca expression, water deficit), and the**

790 **properties of the endophytic Ascomycota communities associated with each**

791 **wood type.**

792 **A**, Mean proportions of healthy wood, black necrosis and white rot for each set of

793 experimental conditions. **B**, Effect of wood type on the alpha-diversity metrics (i.e.

794 observed richness, Shannon and Simpson indices) associated with Ascomycota

795 communities. **C**, PCA summarizing the structure of Ascomycota communities

796 according to an RDA on CLR-transformed data. Ellipses correspond to the 95%
797 interval for each group. **D**, OTUs displaying significant differences in abundance
798 between wood types according to a LeFse analysis. Features with an LDA score > 2
799 and a Kruskal-Wallis *p*-value < 0.05 are shown, and each bar is colored according to
800 the group in which the OTU is overrepresented. **E**, Relative abundance of putative
801 wood pathogens, putative antagonists and other taxa across wood types. All graphs
802 are colored according to wood type.
803

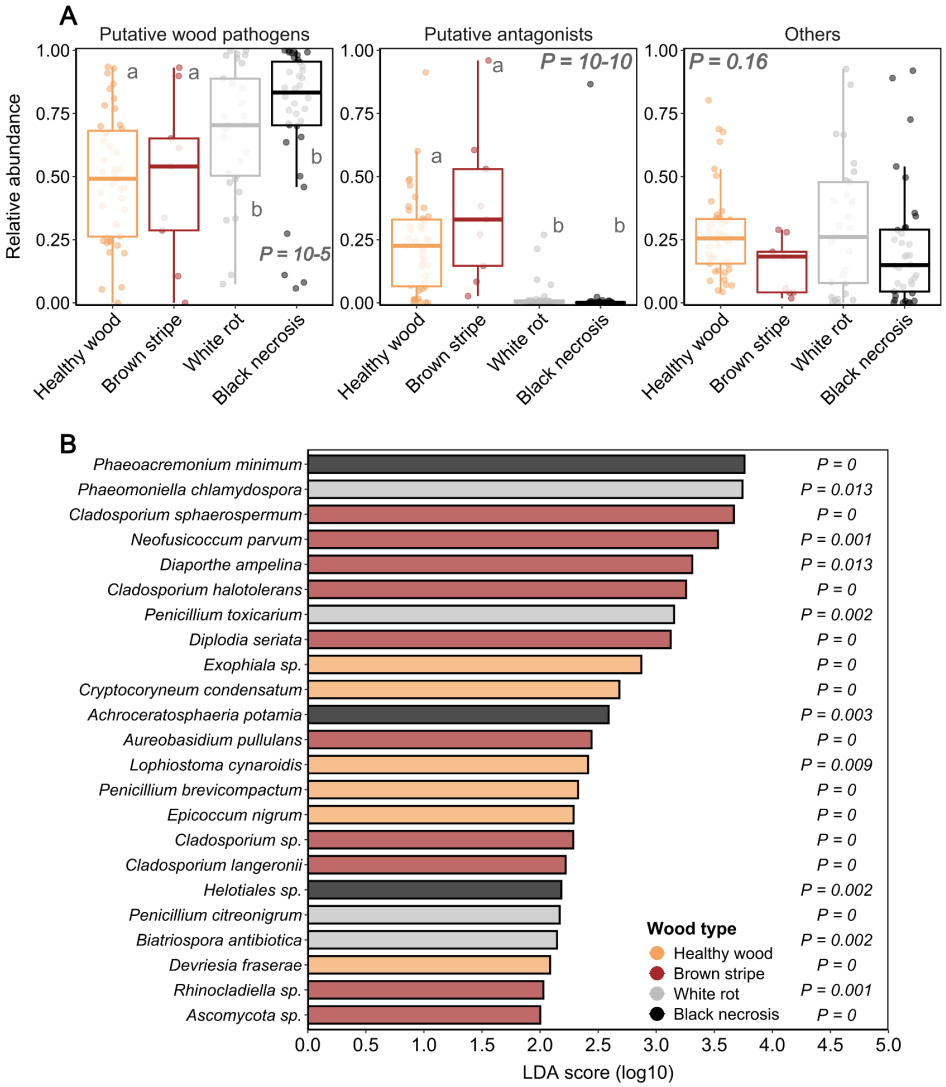

Fig. 4. Functional and taxonomic characterization of Ascomycota communities across wood types. A, Relative abundance of putative wood pathogens, putative antagonists and other taxa, by wood type. All graphs are colored according to wood type. **B**, OTUs with significantly different abundances between wood types according to a LeFse analysis. Features with an LDA score > 2 and a Kruskal-Wallis *p*-value < 0.05 are shown, and each bar is colored according to the group in which the OTU is overrepresented.

812 **Literature cited**

813 Agrios, G. N. 2005. *Plant Pathology, Fifth Edition*. Academic Press.

814 Arnault, G., Mony, C., and Vandenkoornhuyse, P. 2023. Plant microbiota dysbiosis and the
815 Anna Karenina Principle. Trends in Plant Science 28:18–30.
816 https://doi.org/10.1016/j.tplants.2022.08.012.

817 Arbizu PM. 2025. pmartinezarbizu/pairwiseAdonis.

818 Arnold, G., Prado, E., Dumas, V., Butterlin, G., Duchêne, É., Merdinoglu, D., and Avia, K.
819 2025. Discovery of a locus associated with susceptibility to esca in grapevine. Plant Disease.
820 https://doi.org/10.1094/PDIS-06-24-1258-RE.

821 Bakys, R., Vasaitis, R., Barklund, P., Thomsen, I. M., and Stenlid, J. 2009. Occurrence and
822 pathogenicity of fungi in necrotic and non-symptomatic shoots of declining common ash
823 (*Fraxinus excelsior*) in Sweden. Eur J Forest Res 128:51–60. https://doi.org/10.1007/s10342-
824 008-0238-2.

825 Bechtold, E. K., Ryan, S., Moughan, S. E., Ranjan, R., and Nüsslein, K. 2021. Phyllosphere
826 Community Assembly and Response to Drought Stress on Common Tropical and Temperate
827 Forage Grasses. Applied and Environmental Microbiology 87:e00895-21.
828 https://doi.org/10.1128/AEM.00895-21.

829 Bekris, F., Vasileiadis, S., Papadopoulou, E., Samaras, A., Testempasis, S., Gkizi, D., Tavlaki,
830 G., Tzima, A., Paplomatas, E., Markakis, E., Karaoglanidis, G., Papadopoulou, K. K., and
831 Karpouzas, D. G. 2021. Grapevine wood microbiome analysis identifies key fungal pathogens
832 and potential interactions with the bacterial community implicated in grapevine trunk disease
833 appearance. Environmental Microbiome 16:23. https://doi.org/10.1186/s40793-021-00390-1.

834 Bengtsson-Palme, J., Ryberg, M., Hartmann, M., Branco, S., Wang, Z., Godhe, A., De Wit, P.,
835 Sánchez-García, M., Ebersberger, I., de Sousa, F., Amend, A., Jumpponen, A., Unterseher,
836 M., Kristiansson, E., Abarenkov, K., Bertrand, Y. J. K., Sanli, K., Eriksson, K. M., Vik, U.,
837 Veldre, V., and Nilsson, R. H. 2013. Improved software detection and extraction of ITS1 and
838 ITS2 from ribosomal ITS sequences of fungi and other eukaryotes for analysis of

839 environmental sequencing data. Methods in Ecology and Evolution 4:914–919.
840 https://doi.org/10.1111/2041-210X.12073.
841 Bertsch, C., Ramirez-Suero, M., Magnin-Robert, M., Larignon, P., Chong, J., Abou-Mansour,
842 E., Spagnolo, A., Clément, C., and Fontaine, F. 2013. Grapevine trunk diseases: complex and
843 still poorly understood. Plant Pathology 62:243–265. https://doi.org/10.1111/j.1365-
844 3059.2012.02674.x.
845 Bettenfeld, P., Fontaine, F., Trouvelot, S., Fernandez, O., and Courty, P.-E. 2020. Woody
846 Plant Declines. What's Wrong with the Microbiome? Trends in Plant Science 25:381–394.
847 https://doi.org/10.1016/j.tplants.2019.12.024.
848 Bokulich, N. A., Subramanian, S., Faith, J. J., Gevers, D., Gordon, J. I., Knight, R., Mills, D.
849 A., and Caporaso, J. G. 2013. Quality-filtering vastly improves diversity estimates from Illumina
850 amplicon sequencing. Nat Methods 10:57–59. https://doi.org/10.1038/nmeth.2276.
851 Bortolami, G., Farolfi, E., Badel, E., Burlett, R., Cochard, H., Ferrer, N., King, A., Lamarque,
852 L. J., Lecomte, P., Marchesseau-Marchal, M., Pouzoulet, J., Torres-Ruiz, J. M., Trueba, S.,
853 Delzon, S., Gambetta, G. A., and Delmas, C. E. L. 2021a. Seasonal and long-term
854 consequences of esca grapevine disease on stem xylem integrity. Journal of Experimental
855 Botany 72:3914–3928. https://doi.org/10.1093/jxb/erab117.
856 Bortolami, G., Ferrer, N., Baumgartner, K., Delzon, S., Gramaje, D., Lamarque, L. J.,
857 Romanazzi, G., Gambetta, G. A., and Delmas, C. E. L. 2023. Esca grapevine disease involves
858 leaf hydraulic failure and represents a unique premature senescence process. Tree
859 Physiology 43:441–451. https://doi.org/10.1093/treephys/tpac133.
860 Bortolami, G., Gambetta, G. A., Cassan, C., Dayer, S., Farolfi, E., Ferrer, N., Gibon, Y., Jolivet,
861 J., Lecomte, P., and Delmas, C. E. L. 2021b. Grapevines under drought do not express esca
862 leaf symptoms. Proceedings of the National Academy of Sciences 118:e2112825118.
863 https://doi.org/10.1073/pnas.2112825118.
864 Bortolami, G., Gambetta, G. A., Delzon, S., Lamarque, L. J., Pouzoulet, J., Badel, E., Burlett,
865 R., Charrier, G., Cochard, H., Dayer, S., Jansen, S., King, A., Lecomte, P., Lens, F., Torres-
866 Ruiz, J. M., and Delmas, C. E. L. 2019. Exploring the Hydraulic Failure Hypothesis of Esca

867 Leaf Symptom Formation. Plant Physiology 181:1163–1174.
868 https://doi.org/10.1104/pp.19.00591.
869 Broberg, M., Doonan, J., Mundt, F., Denman, S., and McDonald, J. E. 2018. Integrated multi-
870 omic analysis of host-microbiota interactions in acute oak decline. Microbiome 6:21.
871 https://doi.org/10.1186/s40168-018-0408-5.
872 Bruez, E., Vallance, J., Gautier, A., Laval, V., Compant, S., Maurer, W., Sessitsch, A., Lebrun,
873 M.-H., and Rey, P. 2020. Major changes in grapevine wood microbiota are associated with
874 the onset of esca, a devastating trunk disease. Environ Microbiol 22:5189–5206.
875 https://doi.org/10.1111/1462-2920.15180.
876 Bubici, G., and Cirulli, M. 2012. Control of *Verticillium* wilt of olive by resistant rootstocks. Plant
877 Soil 352:363–376. https://doi.org/10.1007/s11104-011-1002-9.
878 Cao Y, Dong Q, Wang D, Zhang P, Liu Y, Niu C. 2022. microbiomeMarker: an R/Bioconductor
879 package for microbiome marker identification and visualization. Bioinformatics 38: 4027–4029.
880 Carbone, M. J., Alaniz, S., Mondino, P., Gelabert, M., Eichmeier, A., Tekielska, D., Bujanda,
881 R., and Gramaje, D. 2021. Drought Influences Fungal Community Dynamics in the Grapevine
882 Rhizosphere and Root Microbiome. Journal of Fungi 7:686.
883 https://doi.org/10.3390/jof7090686.
884 Ciesla, W. M., and Donaubauer, E. 1994. *Decline and Dieback of Trees and Forests: A Global*
885 *Overview*. Food & Agriculture Org.
886 Claverie, M., Lecomte, P., Delorme, G., Dumot, V., Jacquet, O., and Cochard, H. 2023. Xylem
887 water transport is influenced by age and winter pruning characteristics in grapevine (*Vitis*
888 *vinifera*). OENO One 57:53–68. https://doi.org/10.20870/oeno-one.2023.57.3.7452.
889 Claverie, M., Notaro, M., Fontaine, F., and Wery, J. 2020. Current knowledge on Grapevine
890 Trunk Diseases with complex etiology: a systemic approach. Phytopathologia Mediterranea
891 59:29–53. https://doi.org/10.36253/phyto-11150.
892 Compant, S., Samad, A., Faist, H., and Sessitsch, A. 2019. A review on the plant microbiome:
893 Ecology, functions, and emerging trends in microbial application. Journal of Advanced
894 Research 19:29–37. https://doi.org/10.1016/j.jare.2019.03.004.

895 Darriaut, R. C., Marzari, T., Lailheugue, V., Tran, J., Martins, G., Marguerit, E., Isabelle, M.-
896 P., and Lauvergeat, V. 2024. Microbial dysbiosis in roots and rhizosphere of grapevines
897 experiencing decline is associated with active metabolic functions. Front. Plant Sci. 15.
898 https://doi.org/10.3389/fpls.2024.1358213.
899 Darriaut, R., Martins, G., Dewasme, C., Mary, S., Darrieutort, G., Ballestra, P., Marguerit, E.,
900 Vivin, P., Ollat, N., Masneuf-Pomarède, I., and Lauvergeat, V. 2021. Grapevine decline is
901 associated with difference in soil microbial composition and activity. OENO One 55:67.
902 https://doi.org/10.20870/oeno-one.2021.55.3.4626.
903 Darriaut, R., Tran, J., Martins, G., Ollat, N., Masneuf-Pomarède, I., and Lauvergeat, V. 2023.
904 In grapevine decline, microbiomes are affected differently in symptomatic and asymptomatic
905 soils. Applied Soil Ecology 183:104767. https://doi.org/10.1016/j.apsoil.2022.104767.
906 Dayer, S., Lamarque, L. J., Burlett, R., Bortolami, G., Delzon, S., Herrera, J. C., Cochard, H.,
907 and Gambetta, G. A. 2022. Model-assisted ideotyping reveals trait syndromes to adapt
908 viticulture to a drier climate. Plant Physiology 190:1673–1686.
909 https://doi.org/10.1093/plphys/kiac361.
910 Debray, R., Socolar, Y., Kaulbach, G., Guzman, A., Hernandez, C. A., Curley, R., Dhond, A.,
911 Bowles, T., and Koskella, B. 2022. Water stress and disruption of mycorrhizas induce parallel
912 shifts in phyllosphere microbiome composition. New Phytologist 234:2018–2031.
913 https://doi.org/10.1111/nph.17817.
914 de Mendiburu F. 2023. agricolae: Statistical Procedures for Agricultural Research.
915 Del Frari, G., Gobbi, A., Aggerbeck, M. R., Oliveira, H., Hansen, L. H., and Ferreira, R. B.
916 2019. Characterization of the Wood Mycobiome of *Vitis vinifera* in a Vineyard Affected by
917 Esca. Spatial Distribution of Fungal Communities and Their Putative Relation With Leaf
918 Symptoms. Frontiers in Plant Science 10.
919 Del Frari, G., Ingrà, C., Rønne Aggerbeck, M., Gobbi, A., Nascimento, T., Cabral, A., Oliveira,
920 H., Hestbjerg Hansen, L., Ferrandino, A., and Boavida Ferreira, R. 2025. Fungal community
921 dynamics and anthocyanin profiling of grapevine leaves in a vineyard affected by esca. Plant
922 Stress 15:100793. https://doi.org/10.1016/j.stress.2025.100793.

923 Del Frari, G., Oliveira, H., and Boavida Ferreira, R. 2021. White Rot Fungi (Hymenochaetales)
924 and Esca of Grapevine: Insights from Recent Microbiome Studies. J Fungi (Basel) 7:770.
925 https://doi.org/10.3390/jof7090770.
926 Dell'Acqua, N., Gambetta, G. A., Delzon, S., Ferrer, N., Lamarque, L. J., Saurin, N., Theodore,
927 P., and Delmas, C. E. L. 2024. Mechanisms of grapevine resilience to a vascular disease:
928 investigating stem radial growth, xylem development and physiological acclimation. Annals of
929 Botany 133:321–336. https://doi.org/10.1093/aob/mcad188.
930 Dell'Acqua N., Gambetta G.A., Comont G., Ferrer N., Rochepeau A., Petriacq P., Delmas
931 CEL. (2025) Nitrogen nutrition impacts grapevine esca leaf symptom incidence, physiology
932 and metabolism. Journal of Experimental Botany, eraf172 https://doi.org/10.1093/jxb/eraf172
933 Denman, S., Plummer, S., Kirk, S., Peace, A., and McDonald, J. E. 2016. Isolation studies
934 reveal a shift in the cultivable microbiome of oak affected with Acute Oak Decline. Systematic
935 and Applied Microbiology 39:484–490. https://doi.org/10.1016/j.syapm.2016.07.002.
936 Desprez-Loustau, M.-L., Marçais, B., Nageleisen, L.-M., Piou, D., and Vannini, A. 2006.
937 Interactive effects of drought and pathogens in forest trees. Ann. For. Sci. 63:597–612.
938 https://doi.org/10.1051/forest:2006040.
939 Elena, G., Bruez, E., Rey, P., and Luque, J. 2018. Microbiota of grapevine woody tissues with
940 or without esca-foliar symptoms in northeast Spain. Phytopathologia Mediterranea 57:425–
941 438.
942 Escudié, F., Auer, L., Bernard, M., Mariadassou, M., Cauquil, L., Vidal, K., Maman, S.,
943 Hernandez-Raquet, G., Combes, S., and Pascal, G. 2018. FROGS: Find, Rapidly, OTUs with
944 Galaxy Solution. Bioinformatics 34:1287–1294. https://doi.org/10.1093/bioinformatics/btx791.
945 Etienne, L., Fabre, F., Martinetti, D., Frank, E., Michel, L., Bonnardot, V., Guérin-Dubrana, L.,
946 and Delmas, C. E. L. 2024. Exploring the role of cultivar, year and plot age in the incidence of
947 esca and Eutypa dieback: Insights from 20 years of regional surveys in France. Plant
948 Pathology 73:2344–2358. https://doi.org/10.1111/ppa.13975.
949 Farooq, Q. U. A., Hardy, G. E. St. J., McComb, J. A., Thomson, P. C., and Burgess, T. I. 2022.
950 Changes to the Bacterial Microbiome in the Rhizosphere and Root Endosphere of *Persea*

951 *americana* (Avocado) Treated With Organic Mulch and a Silicate-Based Mulch or Phosphite,
952 and Infested With *Phytophthora cinnamomi*. Front Microbiol 13:870900.
953 https://doi.org/10.3389/fmicb.2022.870900.
954 Garcia, J. F., Figueroa-Balderas, R., Comont, G., Delmas, C. E. L., Baumgartner, K., and
955 Cantu, D. 2024. Genome analysis of the esca-associated Basidiomycetes *Fomitiporia*
956 *mediterranea*, *Fomitiporia polymorpha*, *Inonotus vitis*, and *Tropicoporus texanus* reveals
957 virulence factor repertoires characteristic of white-rot fungi. G3 Genes|Genomes|Genetics
958 14:jkae189. https://doi.org/10.1093/g3journal/jkae189.
959 Gastou, P., Irvine, A. D., Arcens, C., Courchinoux, E., This, P., Leeuwen, C. van, and Delmas,
960 C. 2024. Large gradient of susceptibility to esca disease revealed by long-term monitoring of
961 46 grapevine cultivars in a common garden vineyard. OENO One 58.
962 https://doi.org/10.20870/oeno-one.2024.58.2.8043.
963 Gloor, G. B., Macklaim, J. M., Pawlowsky-Glahn, V., and Egozcue, J. J. 2017. Microbiome
964 Datasets Are Compositional: And This Is Not Optional. Front. Microbiol. 8.
965 https://doi.org/10.3389/fmicb.2017.02224.
966 Gómez-Aparicio, L., Domínguez-Begines, J., Villa-Sanabria, E., García, L. V., and Muñoz-
967 Pajares, A. J. 2022. Tree decline and mortality following pathogen invasion alters the diversity,
968 composition and network structure of the soil microbiome. Soil Biology and Biochemistry
969 166:108560. https://doi.org/10.1016/j.soilbio.2022.108560.
970 Gomez-Gallego, M., Galiano, L., Martínez-Vilalta, J., Stenlid, J., Capador-Barreto, H. D.,
971 Elfstrand, M., Camarero, J. J., and Oliva, J. 2022. Interaction of drought- and pathogen-
972 induced mortality in Norway spruce and Scots pine. Plant, Cell & Environment 45:2292–2305.
973 https://doi.org/10.1111/pce.14360.
974 Goodell, B. 2020. Fungi Involved in the Biodeterioration and Bioconversion of Lignocellulose
975 Substrates. In *Genetics and Biotechnology*, eds. J. Philipp Benz and Kerstin Schipper. Cham:
976 Springer International Publishing, pp. 369–397. https://doi.org/10.1007/978-3-030-49924-
977 2_15.

978 Gosling, R. H., Jackson, R. W., Elliot, M., and Nichols, C. P. 2024. Oak declines: Reviewing
979 the evidence for causes, management implications and research gaps. Ecological Solutions
980 and Evidence 5:e12395. https://doi.org/10.1002/2688-8319.12395.
981 Gramaje, D., Úrbez-Torres, J. R., and Sosnowski, M. R. 2018. Managing Grapevine Trunk
982 Diseases With Respect to Etiology and Epidemiology: Current Strategies and Future
983 Prospects. Plant Disease 102:12–39. https://doi.org/10.1094/PDIS-04-17-0512-FE.
984 Griffiths, S. M., Galambao, M., Rowntree, J., Goodhead, I., Hall, J., O'Brien, D., Atkinson, N.,
985 and Antwis, R. E. 2020. Complex associations between cross-kingdom microbial endophytes
986 and host genotype in ash dieback disease dynamics. Journal of Ecology 108:291–309.
987 https://doi.org/10.1111/1365-2745.13302.
988 Guilpart, N., Roux, S., Gary, C., and Metay, A. 2017. The trade-off between grape yield and
989 grapevine susceptibility to powdery mildew and grey mould depends on inter-annual variations
990 in water stress. Agricultural and Forest Meteorology 234–235:203–211.
991 https://doi.org/10.1016/j.agrformet.2016.12.023.
992 Haidar, R., Compant, S., Robert, C., Antonielli, L., Yacoub, A., Grélard, A., Loquet, A., Brader,
993 G., Guyoneaud, R., Attard, E., and Rey, P. 2024. Two *Paenibacillus* spp. strains promote
994 grapevine wood degradation by the fungus *Fomitiporia mediterranea*: from degradation
995 experiments to genome analyses. Sci Rep 14:15779. https://doi.org/10.1038/s41598-024-
996 66620-x.
997 Haidar, R., Yacoub, A., Vallance, J., Compant, S., Antonielli, L., Saad, A., Habenstein, B.,
998 Kauffmann, B., Grélard, A., Loquet, A., Attard, E., Guyoneaud, R., and Rey, P. 2021. Bacteria
999 associated with wood tissues of Esca-diseased grapevines: functional diversity and synergy
1000 with *Fomitiporia mediterranea* to degrade wood components. Environ Microbiol 23:6104–
1001 6121. https://doi.org/10.1111/1462-2920.15676.
1002 Hallmann, J., Quadt-Hallmann, A., Mahaffee, W. F., and Kloepper, J. W. 1997. Bacterial
1003 endophytes in agricultural crops. Can. J. Microbiol. 43:895–914. https://doi.org/10.1139/m97-
1004 131.

1005 Hamaoka, K., Aoki, Y., Takahashi, S., Enoki, S., Yamamoto, K., Tanaka, K., and Suzuki, S.
1006 2022. Diversity of endophytic bacterial microbiota in grapevine shoot xylems varies depending
1007 on wine grape-growing region, cultivar, and shoot growth stage. Sci Rep 12:15772.
1008 https://doi.org/10.1038/s41598-022-20221-8.
1009 Han, G., Mannaa, M., Jeon, H., Jung, H., Kim, J.-C., Park, A. R., and Seo, Y.-S. 2022.
1010 Dysbiosis in the Rhizosphere Microbiome of Standing Dead Korean Fir (*Abies koreana*).
1011 Plants 11:990. https://doi.org/10.3390/plants11070990.
1012 Hofstetter, V., Buyck, B., Croll, D., Viret, O., Couloux, A., and Gindro, K. 2012. What if esca
1013 disease of grapevine were not a fungal disease? Fungal Diversity 54:51–67.
1014 https://doi.org/10.1007/s13225-012-0171-z.
1015 Hrycan, J., Bowen, P., Forge, T., Hart, M., and Úrbez-Torres, J. R. 2025. Impact of water
1016 stress on *Phaeomoniella chlamydospora* abundance and Petri disease symptom development
1017 in young grapevines. OENO One 59. https://doi.org/10.20870/oeno-one.2025.59.1.8317.
1018 Jactel, H., Petit, J., Desprez-Loustau, M.-L., Delzon, S., Piou, D., Battisti, A., and Koricheva,
1019 J. 2012. Drought effects on damage by forest insects and pathogens: a meta-analysis. Global
1020 Change Biology 18:267–276. https://doi.org/10.1111/j.1365-2486.2011.02512.x.
1021 Jaeger, A. C. H., Hartmann, M., Conz, R. F., Six, J., and Solly, E. F. 2024. Drought-induced
1022 tree mortality in Scots pine mesocosms promotes changes in soil microbial communities and
1023 trophic groups. Applied Soil Ecology 194:105198.
1024 https://doi.org/10.1016/j.apsoil.2023.105198.
1025 Jia, S., Yuan, T., Fu, Y., Penuelas, J., Zhou, G., Zhou, L., Liu, D., He, Y., Liu, R., Wang, X.,
1026 Song, B., Jiang, Z., and Zhou, X. 2024. Fungi and bacteria trade-off mediates drought-induced
1027 reduction in wood decomposition. CATENA 243:108169.
1028 https://doi.org/10.1016/j.catena.2024.108169.
1029 Jiao, Z., Gao, Z., Liao, Y., Liu, Y., Dong, L., and Sun, H. 2023. Effects of Pine Wilt Disease on
1030 Rhizosphere Microbiota and Fine Root Fungi: Insights into Enzyme Activity, Ectomycorrhizal
1031 Infection and Microbial Composition. Forests 14:1884. https://doi.org/10.3390/f14091884.

1032 Jiménez-Díaz, R. M., Cirulli, M., Bubici, G., del Mar Jiménez-Gasco, M., Antoniou, P. P., and
1033 Tjamos, E. C. 2012. Verticillium Wilt, A Major Threat to Olive Production: Current Status and
1034 Future Prospects for its Management. Plant Disease 96:304–329.
1035 https://doi.org/10.1094/PDIS-06-11-0496.
1036 Larignon, P., and Dubos, B. 1997. Fungi associated with esca disease in grapevine. European
1037 Journal of Plant Pathology 103:147–157. https://doi.org/10.1023/A:1008638409410.
1038 Larignon, P., Fulchic, R., Cere, L., and Dubos, B. 2001. Observation on black dead arm in
1039 French vineyards. Phytopathologia Mediterranea 40:S336–S342.
1040 Lasa, A. V., Fernández-González, A. J., Villadas, P. J., Mercado-Blanco, J., Pérez-Luque, A.
1041 J., and Fernández-López, M. 2024. Mediterranean pine forest decline: A matter of root-
1042 associated microbiota and climate change. Science of The Total Environment 926:171858.
1043 https://doi.org/10.1016/j.scitotenv.2024.171858.
1044 Leal, C., Bujanda, R., Carbone, M. J., Kiss, T., Eichmeier, A., Gramaje, D., and Maldonado-
1045 González, M. M. 2024. Drought Influences the Structure, Diversity, and Functionality of the
1046 Fungal Community Inhabiting the Grapevine Xylem and Enhances the Abundance of
1047 *Phaeomoniella chlamydospora*. Phytobiomes Journal PBIOMES-02-24-0027-R.
1048 https://doi.org/10.1094/PBIOMES-02-24-0027-R.
1049 Lecomte, P., Bénétreau, C., Diarra, B., Meziani, Y., Delmas, C., and Fermaud, M. 2024.
1050 Logistic modeling of summer expression of esca symptoms in tolerant and susceptible
1051 cultivars in Bordeaux vineyards. OENO One 58. https://doi.org/10.20870/oeno-
1052 one.2024.58.1.7571.
1053 Lecomte, P., Darrieutort, G., Liminana, J.-M., Comont, G., Muruamendiaraz, A., Legorburu,
1054 F.-J., Choueiri, E., Jreijiri, F., El Amil, R., and Fermaud, M. 2012. New Insights into Esca of
1055 Grapevine: The Development of Foliar Symptoms and Their Association with Xylem
1056 Discoloration. Plant Disease 96:924–934. https://doi.org/10.1094/PDIS-09-11-0776-RE.
1057 van Leeuwen, C., Sgubin, G., Bois, B., Ollat, N., Swingedouw, D., Zito, S., and Gambetta, G.
1058 A. 2024. Climate change impacts and adaptations of wine production. Nat Rev Earth Environ
1059 5:258–275. https://doi.org/10.1038/s43017-024-00521-5.

1060 Lin, T., Tang, J., Li, S., Li, S., Han, S., Liu, Y., Yang, C., Chen, G., Chen, L., and Zhu, T. 2023.
1061 Drought stress-mediated differences in phyllosphere microbiome and associated pathogen
1062 resistance between male and female poplars. The Plant Journal 115:1100–1113.
1063 https://doi.org/10.1111/tpj.16283.
1064 Luard, E. J., and Griffin, D. M. 1981. Effect of water potential on fungal growth and turgor.
1065 Transactions of the British Mycological Society 76:33–40. https://doi.org/10.1016/S0007-
1066 1536(81)80006-X.
1067 Luna, I. J., Santiago, L., Ezcurra, E., Xi, M., Ashworth, V. E. T. M., Nothnagel, E., and
1068 Rolshausen, P. E. 2025. Physiological symptoms induced by drought stress outweigh vascular
1069 pathogen infection in walnut. Tree Physiology 45:tpaf034.
1070 https://doi.org/10.1093/treephys/tpaf034.
1071 Ma, Y., Shen, Y., Zhou, X., Ma, H., Lan, J., Fu, B., and Xue, Q. 2024. Biological Decline of
1072 Alfalfa Is Accompanied by Negative Succession of Rhizosphere Soil Microbial Communities.
1073 Plants 13:2589. https://doi.org/10.3390/plants13182589.
1074 Magnin-Robert, M., Adrian, M., Trouvelot, S., Spagnolo, A., Jacquens, L., Letousey, P.,
1075 Rabenoelina, F., Harir, M., Roullier-Gall, C., Clément, C., Schmitt-Kopplin, P., Vallat, A., Abou-
1076 Mansour, E., and Fontaine, F. 2017. Alterations in Grapevine Leaf Metabolism Occur Prior to
1077 Esca Apoplexy Appearance. MPMI 30:946–959. https://doi.org/10.1094/MPMI-02-17-0036-R.
1078 Magnin-Robert, M., Spagnolo, A., Boulanger, A., Joyeux, C., Clément, C., Abou-Mansour, E.,
1079 and Fontaine, F. 2016. Changes in Plant Metabolism and Accumulation of Fungal Metabolites
1080 in Response to Esca Proper and Apoplexy Expression in the Whole Grapevine.
1081 Phytopathology® 106:541–553. https://doi.org/10.1094/PHYTO-09-15-0207-R.
1082 Mahé, F., Rognes, T., Quince, C., Vargas, C. de, and Dunthorn, M. 2014. Swarm: robust and
1083 fast clustering method for amplicon-based studies. PeerJ 2:e593.
1084 https://doi.org/10.7717/peerj.593.
1085 Maher, N., Piot, J., Bastien, S., Vallance, J., Rey, P., and Guérin-Dubrana, L. 2012. Wood
1086 necrosis in esca-affected vines: types, relationships and possible links with foliar symptom
1087 expression. OENO One 46:15–27. https://doi.org/10.20870/oeno-one.2012.46.1.1507.

1088 Manion, P. D. 1981. *Tree disease concepts*. Englewood Cliffs, N.J: Prentice-Hall.
1089 Marsberg, A., Kemler, M., Jami, F., Nagel, J. H., Postma-Smidt, A., Naidoo, S., Wingfield, M.
1090 J., Crous, P. W., Spatafora, J. W., Hesse, C. N., Robbertse, B., and Slippers, B. 2017.
1091 *Botryosphaeria dothidea*: a latent pathogen of global importance to woody plant health.
1092 Molecular Plant Pathology 18:477–488. https://doi.org/10.1111/mpp.12495.
1093 Martín, L., García-García, B., and Alguacil, M. del M. 2022. Interactions of the Fungal
1094 Community in the Complex Patho-System of Esca, a Grapevine Trunk Disease. International
1095 Journal of Molecular Sciences 23:14726. https://doi.org/10.3390/ijms232314726.
1096 Martin, M. 2011. Cutadapt removes adapter sequences from high-throughput sequencing
1097 reads. EMBnet.journal 17:10–12. https://doi.org/10.14806/ej.17.1.200.
1098 McElrone, A. J., Manuck, C. M., Brodersen, C. R., Patakas, A., Pearsall, K. R., and Williams,
1099 L. E. 2021. Functional hydraulic sectoring in grapevines as evidenced by sap flow, dye
1100 infusion, leaf removal and micro-computed tomography. AoB PLANTS 13:plab003.
1101 https://doi.org/10.1093/aobpla/plab003.
1102 McMurdie, P. J., and Holmes, S. 2013. phyloseq: An R Package for Reproducible Interactive
1103 Analysis and Graphics of Microbiome Census Data. PLOS ONE 8:e61217.
1104 https://doi.org/10.1371/journal.pone.0061217.
1105 Monod, V., Hofstetter, V., Viret, O., Zufferey, V., Gindro, K., and Croll, D. 2024. Landscape-
1106 scale endophytic community analyses in replicated grapevine stands reveal that dieback
1107 disease is not caused by specific fungal communities. 2024.04.05.588363.
1108 https://doi.org/10.1101/2024.04.05.588363.
1109 Morales-Cruz, A., Allenbeck, G., Figueroa-Balderas, R., Ashworth, V. E., Lawrence, D. P.,
1110 Travadon, R., Smith, R. J., Baumgartner, K., Rolshausen, P. E., and Cantu, D. 2018a. Closed-
1111 reference metatranscriptomics enables in planta profiling of putative virulence activities in the
1112 grapevine trunk disease complex. Molecular Plant Pathology 19:490–503.
1113 https://doi.org/10.1111/mpp.12544.
1114 Morales-Cruz, A., Figueroa-Balderas, R., García, J. F., Tran, E., Rolshausen, P. E.,
1115 Baumgartner, K., and Cantu, D. 2018b. Profiling grapevine trunk pathogens in planta: a case

1116 for community-targeted DNA metabarcoding. BMC Microbiology 18:214.
1117 https://doi.org/10.1186/s12866-018-1343-0.
1118 Moretti, S., Goddard, M.-L., Puca, A., Lalevée, J., Di Marco, S., Mugnai, L., Gelhaye, E.,
1119 Goodell, B., Bertsch, C., and Farine, S. 2023. First Description of Non-Enzymatic Radical-
1120 Generating Mechanisms Adopted by *Fomitiporia mediterranea*: An Unexplored Pathway of the
1121 White Rot Agent of the Esca Complex of Diseases. Journal of Fungi 9:498.
1122 https://doi.org/10.3390/jof9040498.
1123 Moretti, S., Pacetti, A., Pierron, R., Kassemeyer, H.-H., Fischer, M., Péros, J.-P., Perez-
1124 Gonzalez, G., Bieler, E., Schilling, M., Marco, S. D., Gelhaye, E., Mugnai, L., Bertsch, C., and
1125 Farine, S. 2021. Fomitiporia mediterranea M. Fisch., the historical Esca agent: a
1126 comprehensive review on the main grapevine wood rot agent in Europe. Phytopathologia
1127 Mediterranea 60:351–379. https://doi.org/10.36253/phyto-13021.
1128 Nerva, L., Garcia, J. F., Favaretto, F., Giudice, G., Moffa, L., Sandrini, M., Cantu, D., Zanzotto,
1129 A., Gardiman, M., Velasco, R., Gambino, G., and Chitarra, W. 2022. The hidden world within
1130 plants: metatranscriptomics unveils the complexity of wood microbiomes. J Exp Bot 73:2682–
1131 2697. https://doi.org/10.1093/jxb/erac032.
1132 Oksanen J, Simpson GL, Blanchet FG, Kindt R, Legendre P, Minchin PR, O'Hara RB, Solymos
1133 P, Stevens MHH, Szoecs E, et al. 2022. vegan: Community Ecology Package.
1134 Ouadi, L., Bruez, E., Bastien, S., Vallance, J., Lecomte, P., Domec, J.-C., and Rey, P. 2019.
1135 Ecophysiological impacts of Esca, a devastating grapevine trunk disease, on *Vitis vinifera* L.
1136 PLOS ONE 14:e0222586. https://doi.org/10.1371/journal.pone.0222586.
1137 Pacetti, A., Moretti, S., Pinto, C., Compant, S., Farine, S., Bertsch, C., and Mugnai, L. 2021.
1138 Trunk Surgery as a Tool to Reduce Foliar Symptoms in Diseases of the Esca Complex and
1139 Its Influence on Vine Wood Microbiota. Journal of Fungi 7:521.
1140 https://doi.org/10.3390/jof7070521.
1141 Raghavendra, A. K. H., Bissett, A. B., Thrall, P. H., Morin, L., Steinrucken, T. V., Galea, V. J.,
1142 Goulter, K. C., and van Klinken, R. D. 2017. Characterisation of above-ground endophytic and

1143 soil fungal communities associated with dieback-affected and healthy plants in five exotic
1144 invasive species. Fungal Ecology 26:114–124. https://doi.org/10.1016/j.funeco.2017.01.003.
1145 Ramegowda, V., and Senthil-Kumar, M. 2015. The interactive effects of simultaneous biotic
1146 and abiotic stresses on plants: mechanistic understanding from drought and pathogen
1147 combination. J Plant Physiol 176:47–54. https://doi.org/10.1016/j.jplph.2014.11.008.
1148 Riou, C., Agostini, D., Aigrain, P., Barthe, M., Robert, M.-L. des, Gervais, J.-P., Jobard, E.,
1149 Lurton, L., Moncomble, D., and Prêtet-Lataste, C. 2016. Action plan against declining
1150 vineyards: An innovative approach. BIO Web Conf. 7:01040.
1151 https://doi.org/10.1051/bioconf/20160701040.
1152 Schilling, M., Maia-Grondard, A., Baltenweck, R., Robert, E., Hugueney, P., Bertsch, C.,
1153 Farine, S., and Gelhaye, E. 2022. Wood degradation by *Fomitiporia mediterranea* M. Fischer:
1154 Physiologic, metabolomic and proteomic approaches. Front Plant Sci 13:988709.
1155 https://doi.org/10.3389/fpls.2022.988709.
1156 Schneider, C. A., Rasband, W. S., and Eliceiri, K. W. 2012. NIH Image to ImageJ: 25 years of
1157 image analysis. Nat Methods 9:671–675. https://doi.org/10.1038/nmeth.2089.
1158 Skovsgaard, J. P., Thomsen, I. M., Skovgaard, I. M., and Martinussen, T. 2010. Associations
1159 among symptoms of dieback in even-aged stands of ash (*Fraxinus excelsior* L.). Forest
1160 Pathology 40:7–18. https://doi.org/10.1111/j.1439-0329.2009.00599.x.
1161 Solís-García, I. A., Ceballos-Luna, O., Cortazar-Murillo, E. M., Desgarennes, D., Garay-
1162 Serrano, E., Patiño-Conde, V., Guevara-Avendaño, E., Méndez-Bravo, A., and Reverchon, F.
1163 2021. Phytophthora Root Rot Modifies the Composition of the Avocado Rhizosphere
1164 Microbiome and Increases the Abundance of Opportunistic Fungal Pathogens. Front.
1165 Microbiol. 11. https://doi.org/10.3389/fmicb.2020.574110.
1166 Steinrucken, T. V., Bissett, A., Powell, J. R., Raghavendra, Anil. K. H., and van Klinken, R. D.
1167 2016. Endophyte community composition is associated with dieback occurrence in an invasive
1168 tree. Plant Soil 405:311–323. https://doi.org/10.1007/s11104-015-2529-y.

1169 Surico, G., Mugnai, L., and Marchi, G. 2006. Older and More Recent Observations on Esca :
1170 A Critical Overview. Phytopathologia Mediterranea 68–86.
1171 https://doi.org/10.14601/Phytopathol_Mediterr-1847.
1172 Torres-Ruiz, J. M., Cochard, H., Delzon, S., Boivin, T., Burlett, R., Cailleret, M., Corso, D.,
1173 Delmas, C. E. L., De Caceres, M., Diaz-Espejo, A., Fernández-Conradi, P., Guillemot, J.,
1174 Lamarque, L. J., Limousin, J.-M., Mantova, M., Mencuccini, M., Morin, X., Pimont, F., De Dios,
1175 V. R., Ruffault, J., Trueba, S., and Martin-StPaul, N. K. 2024. Plant hydraulics at the heart of
1176 plant, crops and ecosystem functions in the face of climate change. New Phytologist 241:984–
1177 999. https://doi.org/10.1111/nph.19463.
1178 Trivedi, P., Batista, B. D., Bazany, K. E., and Singh, B. K. 2022. Plant–microbiome interactions
1179 under a changing world: responses, consequences and perspectives. New Phytologist
1180 234:1951–1959. https://doi.org/10.1111/nph.18016.
1181 Trivedi, P., Leach, J. E., Tringe, S. G., Sa, T., and Singh, B. K. 2020. Plant–microbiome
1182 interactions: from community assembly to plant health. Nat Rev Microbiol 18:607–621.
1183 https://doi.org/10.1038/s41579-020-0412-1.
1184 Weiller, F., Diniz, I., Pimentel, D., Erban, A., Reis, P., Soares, F., Rego, C., Kopka, J., and
1185 Fortes, A. M. 2024. Metabolomic analysis of grapes and leaves from symptomatic and
1186 asymptomatic *Vitis vinifera* grapevines with Esca disease. Current Plant Biology 40:100378.
1187 https://doi.org/10.1016/j.cpb.2024.100378.
1188 Xu, L., Naylor, D., Dong, Z., Simmons, T., Pierroz, G., Hixson, K. K., Kim, Y.-M., Zink, E. M.,
1189 Engbrecht, K. M., Wang, Y., Gao, C., DeGraaf, S., Madera, M. A., Sievert, J. A., Hollingsworth,
1190 J., Birdseye, D., Scheller, H. V., Hutmacher, R., Dahlberg, J., Jansson, C., Taylor, J. W.,
1191 Lemaux, P. G., and Coleman-Derr, D. 2018. Drought delays development of the sorghum root
1192 microbiome and enriches for monoderm bacteria. Proceedings of the National Academy of
1193 Sciences 115:E4284–E4293. https://doi.org/10.1073/pnas.1717308115.
1194 Zabel, R. A., and Morrell, J. J. 2012. *Wood Microbiology: Decay and Its Prevention*. Academic
1195 Press.

1196 Zinger, L., Lionnet, C., Benoiston, A.-S., Donald, J., Mercier, C., and Boyer, F. 2021. metabaR:
1197 An r package for the evaluation and improvement of DNA metabarcoding data quality.
1198 Methods in Ecology and Evolution 12:586–592. https://doi.org/10.1111/2041-210X.13552.